Bioorganic Chemistry 87 (2019) 380–394

Contents lists available at ScienceDirect

Bioorganic Chemistry

journal homepage: www.elsevier.com/locate/bioorg

Novel 8-amino-1,2,4-triazolo[4,3-*a*]pyrazin-3-one derivatives as potent human adenosine A_1 and A_{2A} receptor antagonists. Evaluation of their protective effect against β-amyloid-induced neurotoxicity in SH-SY5Y cells

Matteo Falsini[a], Daniela Catarzi[a], Flavia Varano[a], Diego Dal Ben[b], Gabriella Marucci[b], Michela Buccioni[b], Rosaria Volpini[b], Lorenzo Di Cesare Mannelli[c], Carla Ghelardini[c], Vittoria Colotta[a,*]

[a] Dipartimento di Neuroscienze, Psicologia, Area del Farmaco e Salute del Bambino, Sezione di Farmaceutica e Nutraceutica, Università degli Studi di Firenze, Via Ugo Schiff, 6, 50019 Sesto Fiorentino, Italy
[b] Scuola di Scienze del Farmaco e dei Prodotti della Salute, Università degli Studi di Camerino, via S. Agostino 1, 62032 Camerino, MC, Italy
[c] Dipartimento di Neuroscienze, Psicologia, Area del Farmaco e Salute del Bambino, Sezione di Farmacologia, Università degli Studi di Firenze, Viale Pieraccini 5, 50139 Firenze, Italy

ARTICLE INFO

Keywords:
G protein-coupled receptors
Adenosine receptors
Adenosine receptor antagonists
1,2,4-triazolo[4,3-a]pyrazin-3-ones
Alzheimer disease
Ligand-adenosine receptor modeling studies

ABSTRACT

In this work, an enlarged series of 1,2,4-triazolo[4,3-*a*]pyrazin-3-ones was designed to target the human (h) A_{2A} adenosine receptor (AR) or both hA_1 and hA_{2A} ARs. The novel 8-amino-1,2,4-triazolopyrazin-3-one derivatives **1–25** featured a phenyl or a benzyl pendant at position 2 while different aryl/heteroaryl substituents were placed at position 6. Two compounds (**8** and **10**) endowed with high affinity (K_i = 7.2 and 10.6 nM) and a complete selectivity for the hA_{2A} AR were identified. Moreover, several derivatives possessed nanomolar affinity for both hA_1 and hA_{2A} ARs (both K_i < 20 nM) and different degrees of selectivity versus the hA_3 AR. Two selected compounds (**10** and **25**) demonstrated ability in preventing β-amyloid peptide (25–35)-induced neurotoxicity in SH-SY5Y cells. Results of docking studies at the hA_{2A} and hA_1 AR crystal structures helped us to rationalize the observed affinity data and to highlight that the steric hindrance of the substituents at the 2- and 6-position of the bicyclic core affects the binding mode in the receptor cavity.

1. Introduction

Adenosine is a ubiquitous neuromodulator which controls many physiological and pathological processes, both in the central and peripheral nervous system. Adenosine exerts its effects through activation of G protein-coupled receptors, subdivided into the four subtypes A_1, A_{2A}, A_{2B} and A_3 [1,2]. A_1 and A_3 adenosine receptors (ARs) are negatively coupled to adenylate cyclase while A_{2A} and A_{2B} subtypes activate the enzyme. The hA_1 AR subtype is the most abundant in the brain and is traditionally considered a neuroprotective receptor due to its inhibitory effects [3]. For instance, it curtails excitatory neurotransmission thus exerting a protective role in diverse pathological conditions linked to glutamate excitotoxicity such as cerebral ischemia or epilepsy. Nevertheless, there is recent evidence that A_1 AR-sustained activation after stroke or ischemia induces AMPA receptor endocytosis and the consequent, persistent synaptic depression may contribute to enhanced neuronal death [4–6].

The hA_{2A} AR subtype has less widespread localization at central level where it shows higher density in the basal ganglia and lower in the cortex and hippocampus. Blockade of this AR subtype exerts a protective effect in different models of cerebral ischemia and neurodegenerative disorders, such as Parkinson's or Alzheimer's diseases [4,7–16]. In the last decade, several human studies have highlighted that consumption of caffeine, a non-selective A_1 and A_{2A} AR antagonist, negatively correlated with the risk of developing AD and PD [9,11,12]. The protective effect of caffeine, investigated in animal models of AD and PD was ascribed to antagonism of the A_{2A} AR subtype, among other pathways [10–14]. Related to AD models, both caffeine and the potent A_{2A} AR antagonist ZM 241,385 (4-(2-[7-amino-2-(2-furyl)-1,2,4-triazolo[2,3-*a*]triazin-5-ylamino]ethyl]phenol) prevented cell death after exposure of rat cultured cerebellar granule neurons to the β-amyloid peptide (25–35) [13]. A_{2A} AR antagonists demonstrated an ability to alleviate cognitive deficits caused by administration of the β-amyloid peptides in different *in vivo* rodent models [14,15]. However, more

* Corresponding author.
E-mail address: vittoria.colotta@unifi.it (V. Colotta).

https://doi.org/10.1016/j.bioorg.2019.03.046
Received 4 September 2018; Received in revised form 13 December 2018; Accepted 15 March 2019
Available online 16 March 2019

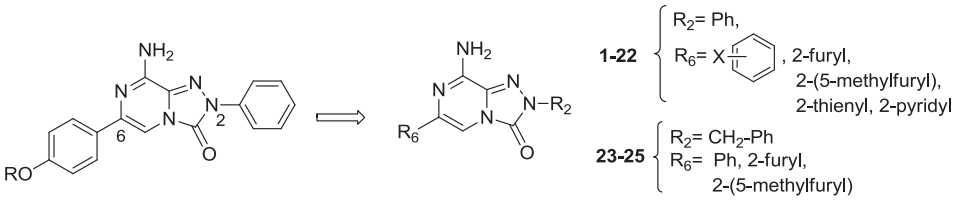

Fig. 1. Previously and currently reported 1,2,4-triazolo[4,3-*a*]pyrazin-3-ones **1–25**.

recently, also A_1 AR antagonism was recognized as affording neuroprotection in a model of combined neurotoxicity. In fact, the protective effect of dual A_1 and A_{2A} AR blockade in preventing β-amyloid toxicity in neuroblastoma cells exposed to aluminium chloride was demonstrated [16].

In recent years, as part of a research program aimed at finding new adenosine receptor antagonists [17–25], we disclosed the 8-amino-1,2,4-triazolo[4,3-*a*]pyrazin-3-one as a new decorable scaffold to obtain potent antagonists able to bind selectively the hA_{2A} AR or both the hA_1 and hA_{2A} subtypes [21] (Fig. 1). The SAR study showed that the unsubstituted phenyl ring at position 2 was the best group for obtaining an efficient hA_{2A} receptor interaction, and that the presence of small para alkoxy groups (OMe, OEt, O-isopropyl, O-propargyl) on the 6-phenyl pendant afforded nanomolar affinity and a complete selectivity for this AR subtype.

To continue investigations of the 8-amino-1,2,4-triazolopyrazin-3-one series, we designed and synthesized an enlarged series of derivatives to obtain antagonists for the hA_{2A} AR or both hA_1 and hA_{2A} ARs. These types of ligands were of our interest for their ability to induce neuroprotection in different neurodegenerative diseases. Thus, a new set of triazolopyrazines, featuring the unsubstituted phenyl ring at position 2 and heteroaryl or aryl groups at position 6 (Fig. 1 compounds **1–22**), were synthesized. Simple substituents, endowed with different electronic, steric and lipophilic properties, were probed on the 6-phenyl ring (X = OMe, NO_2, NH_2, Br, Cl). The NH_2 group was also inserted to construct the piperazine moiety appended on the 6-phenyl moiety (compounds **17–22**). Finally, derivatives featuring a benzyl chain at position 2 and a phenyl ring or a 2-furyl/2-(5-methylfuryl) group at position 6 were synthesized (derivatives **23–25**) since the benzyl pendant and the furyl moiety were thought to enhance compound solubility.

2. Results and discussion

2.1. Chemistry

The new 8-amino-1,2,4-triazolo[4,3-*a*]pyrazin-3-one derivatives **1–25** were prepared as described in Schemes 1–3. Scheme 1 depicts the synthesis of the 2-phenyl derivatives **1–16** which were obtained starting from ethyl 1-phenyl-5-oxo-1H-1,2,4-triazole-3-carboxylate **26** [21].

N^4-Alkylation of **26** with the suitable α-aloketones in DMF/CH_3CN, and in the presence of potassium carbonate, afforded the ethyl −5-oxo-4-phenyl-1,2,4-triazole-3-carboxylate derivatives **27–38** whose cyclization with ammonium acetate, in a sealed tube at 150 °C, gave the 2-phenyl-1,2,4-triazolo[4,3-*a*]pyrazine-3,8-diones **39–50**. The 6-(2-methoxyphenyl) derivative **43** was demethylated with BBr_3 to yield the corresponding hydroxy-substituted compound **51**. Catalytic (Pd/C) hydrogenation of the meta- and para-nitro derivatives **45–46**, in a Parr apparatus, furnished the respective amino-substituted compounds **52–53**. The 3,8-diones **39–50** were chlorinated with phosphorus oxychloride, under microwave irradiation, to obtain the corresponding 8-chloro derivatives **54–65** which gave the desired 8-amino-1,2,4-triazolo[4,3-*a*]pyrazin-3-ones **1–12** upon treatment with a saturated solution of ammonia in absolute ethanol. Demethylation of the 6-(2-methoxyphenyl) derivative **5** with BBr_3 gave the corresponding 6-(2-hydroxyphenyl)-substituted compound **13**. The nitro derivatives **6–8** were reduced (H_2, Pd/C) in a Parr apparatus to yield the corresponding

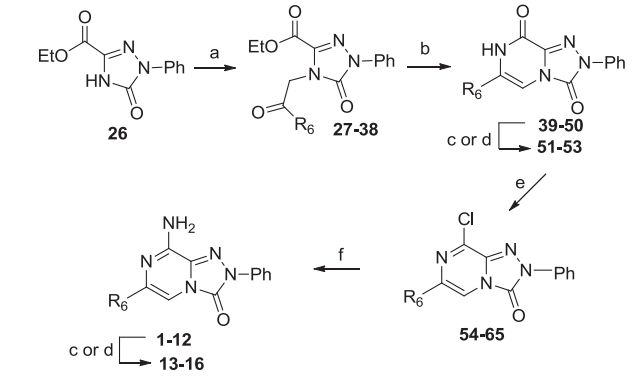

	R_6		R_6
1, 27, 39, 54	2-furyl	**9, 35, 47, 62**	C_6H_4-3-Br
2, 28, 40, 55	2-(5-methylfuryl)	**10, 36, 48, 63**	C_6H_4-4-Br
3, 29, 41, 56	2-thienyl	**11, 37, 49, 64**	C_6H_4-3-Cl
4, 30, 42, 57	2-pyridyl	**12, 38, 50, 65**	C_6H_4-4-Cl
5, 31, 43, 58	C_6H_4-2-OCH_3	**13, 51**	C_6H_4-2-OH
6, 32, 44, 59	C_6H_4-2-NO_2	**14**	C_6H_4-2-NH_2
7, 33, 45, 60	C_6H_4-3-NO_2	**15, 52**	C_6H_4-3-NH_2
8, 34, 46, 61	C_6H_4-4-NO_2	**16, 53**	C_6H_4-4-NH_2

Scheme 1. Reagents and conditions: (a) R_6-$COCH_2Br$, K_2CO_3, DMF/CH_3CN, rt; (b) NH_4OAc, 150 °C sealed tube; (c) from **43, 5**, BBr_3, anhydrous CH_2Cl_2, 0 °C-rt; (d) from **45, 46, 6–8**, H_2, Pd/C, DMF, Parr apparatus, 40 psi; (e) $POCl_3$, mw or conventional heating, 140–180 °C; (f) NH_3, absolute EtOH.

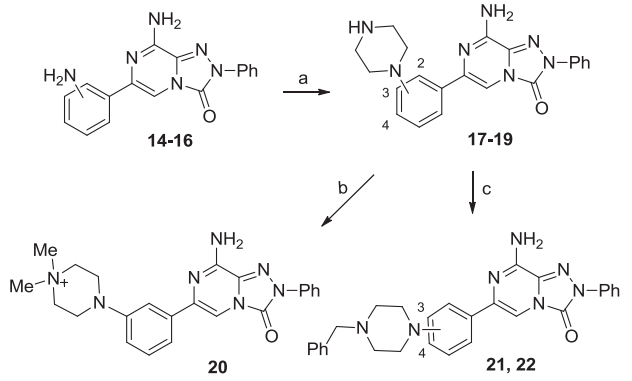

Scheme 2. Reagents and conditions: (a) (i) Bis(2-chloroethyl)amine hydrochloride, sulfolane, 150 °C, (ii) $NaHCO_3$ saturated solution; (b) CH_3I, anhydrous DMF, rt; (c) $PhCH_2Br$, Et_3N, anhydrous 1,4-dioxane, reflux.

amino derivatives **14–16**. Synthesis of the triazolopyrazines **17–22**, featuring a piperazine on the 6-phenyl pendant, is outlined in Scheme 2.

The piperazine ring was constructed by alkylation of the aromatic amino group of derivatives **14–16** with bis(2-chloroethyl)amine in sulfolane at 150 °C. Reaction of the 6-(3-piperazin-1-yl)-substituted compound **18** with methyl iodide gave rise to the N,N-dimethylpiperazinium salt **20**. Compounds **18** and **19** were reacted with benzyl bromide to obtain the respective N-benzylpiperazin-1-yl-derivatives **21** and **22**.

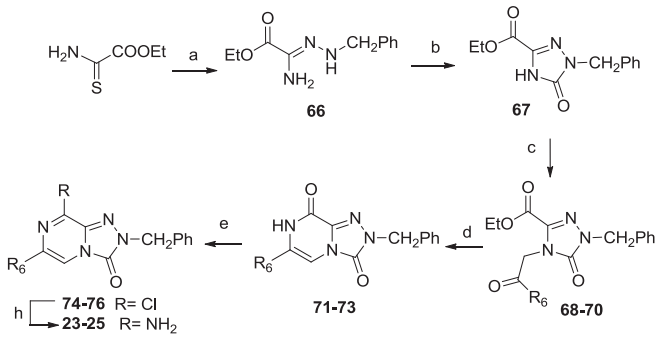

	R_6
23, 68, 71, 74	Ph
24, 69, 72, 75	2-furyl
25, 70, 73, 76	2-(5-methylfuryl)

Scheme 3. Reagents and conditions: (a) Benzylhydrazine dihydrochloride, absolute EtOH, K_2CO_3, rt; (b) carbonyldiimidazole, CH_2Cl_2, rt; (c) R_6-$COCH_2Br$, K_2CO_3, DMF/CH_3CN, rt; (d) NH_4OAc, 150 °C sealed tube; (g) $POCl_3$, mw or conventional heating, 140–180 °C; (h) NH_3, absolute EtOH.

The 2-benzyl-substituted 1,2,4-triazolo[4,3-*a*]pyrazin-3-one derivatives **23–25** were synthesized as drawn in Scheme 3, i.e. starting from ethyl 2-amino-2-(2-benzyl-hydrazono)acetate **66.** The latter was obtained by reacting ethyl 2-amino-2-thioxoacetate with benzylhydrazine dihydrochloride, in absolute ethanol and in the presence of potassium carbonate. Compound **66** was then cyclized with carbonyldiimidazole to give the key intermediate 2-benzyl-5-oxotriazole derivative **67** which was transformed into the desired the 2-benzyl-triazolo[4,3-*a*]pyrazine derivatives **23–25** through the same pathway described above to prepare **1–16**.

2.2. Binding and cAMP assays

The 8-amino-1,2,4-triazolo[4,3-*a*]pyrazin-3-ones **1–25** were evaluated for their affinity to hA_1, hA_{2A} and hA_3 ARs, stably transfected in Chinese hamster ovary (CHO) cells, and were also tested at the hA_{2B} AR subtype by measuring their inhibitory effects on 5′-(N-ethyl-carboxamido)adenosine (NECA)-stimulated cAMP levels in hA_{2B} CHO cells. The selected derivatives **10**, **11** and **25**, showing high affinity for hA_1 and/or hA_{2A} ARs, were investigated to determine their antagonistic potency by measuring their effects on cAMP production in CHO cells, stably expressing hA_1 or hA_{2A} ARs. Biological studies were also carried out on the 3,8-dione derivatives **39–53, 71–73** because they were thought to possess some affinity for the hA_3 AR subtype, which was still of our interest even though being off-target for the work. The results of binding and cAMP assays are presented in Tables 1–3, where the data of the previously reported 2,6-diphenyl-1,2,4-triazolopirazine derivatives **A** [21] (Table 1) and **B** [21] (Table 2) are also included as references.

2.3. Structure-affinity relationship studies

The biological data of the 8-amino-1,2,4-triazolo[4,3-*a*]pyrazin-3-ones **1–25** (Table 1) show that the structural modifications carried out on 2,6-diphenyl-substituted derivative **A**, an equally potent ligand on hA_1, hA_{2A} and hA_3 ARs (K_i = 10–13 nM), shifted affinity toward the A_1 and A_{2A} ARs. Two new derivatives (**8** and **10**) possess high hA_{2A} affinity and selectivity and most compounds bind both the hA_1 and hA_{2A} ARs with nanomolar affinity, while showing different degrees of selectivity versus the hA_3 subtype. Among the latter derivatives, the best in terms of hA_{2A} affinity were **5**, **13** and **24**, displaying K_i values in the range of 2–2.4 nM.

Concerning the hA_{2B} AR, compounds **1–25** were inactive (IC_{50} > 30,000 nM) in inhibiting the NECA-stimulated cAMP levels in hA_{2B} CHO cells, thus it can be deduced that they lacked affinity for the hA_{2B} AR.

Replacement of the 6-phenyl ring of the reference ligand **A** with a heterocyclic moiety (compounds **2–4**) maintained a high affinity for both hA_1 and hA_{2A} ARs (K_i = 8.4–13.2 nM) while enhancing selectivity versus the hA_3 subtype.

Substituents possessing different lipophilicity, electronic and steric properties (OMe, OH, NO_2, NH_2, Cl, Br) were then probed on the 6-phenyl ring. When a methoxy or a hydroxy group was introduced on the ortho position of the 6-phenyl ring of compound **A**, to give derivatives **5** and **13**, respectively, quite similar affinity profiles were obtained, notwithstanding the different properties of the two groups, e.g. lipophilicity or ability to engage H bonding. Both compounds showed in fact high affinity for the hA_{2A} AR (K_i about 2 nM) and lower, but still nanomolar, affinities for the hA_1 and hA_3 ARs.

Introduction of a 4-nitro and a 4-bromo substituent on the 6-phenyl ring resulted in potent and selective hA_{2A} antagonists (compounds **8** and **10**, respectively, K_i = 7.2 and 8.1 nM). Insertion of the nitro group to the ortho position yielded derivative **6**, which showed moderate affinity for the hA_1, hA_{2A} and hA_3 ARs. For the meta nitro-substituted derivative **7**, good hA_1 and hA_3 AR affinities were achieved (K_i = 35.9 and 38.6 nM, respectively) while it was not possible to obtain the hA_{2A} data. Its low solubility in the assay medium did not allow it to reach high enough concentrations to obtain the dose–response curve. Introduction of the lipophilic 3-bromo (**9**), 3-chloro (**11**) and 4-chloro (**12**) substituent on the 6-phenyl moiety led to potent and dual hA_1 and hA_{2A} ligands (K_i = 4.71–14.3 nM). The hydrophilic amino group inserted either in meta (**15**) or para (**16**) position gave compounds able to bind efficiently (K_i = 10.9–33.5 nM) both hA_1 and hA_{2A} ARs while the same group at the ortho position (**14**) preserved the hA_{2A} affinity (K_i = 19.5 nM) but worsened the hA_1 one (K_i = 191 nM). All three amino-substituted compounds **14–16** showed also some ability to bind the hA_3 receptor subtype.

Introduction of substituted piperazine moieties on the 6-phenyl group (**17–22**) was pursued since these residues are a common feature of known potent and selective hA_{2A} AR antagonists, structurally correlated to our series [26], and are also a useful group for improving the drug-likeness of the compounds. On the whole, this kind of modification was not as profitable as expected, in terms of hA_{2A} affinity. Insertion of an unsubstituted piperazine at the ortho position made the compound (**17**) a very weak ligand at all ARs, while its presence at the para position (**19**) permitted a quite good and selective interaction with the hA_{2A} AR. Unfortunately, we were not able to determine the hA_{2A} AR affinity of the meta- piperazine derivative **18** due to the problems described above for compound **7**. The N,N-dimethylation of the meta-piperazine group afforded a quite good affinity for the hA_{2A} AR (**20**), and an even better substitution was the N-benzylation of the meta- (**21**) or para- (**22**) piperazine, giving rise to low nanomolar affinities at this receptor.

Derivatives **23–25**, bearing a benzyl chain at position 2, combined with a phenyl, 2-furyl and a 2-(5-methylfuryl) at position 6, were synthesized because the benzyl pendant, being more flexible than the 2-phenyl moiety, was thought to enhance the solubility of the compounds. Moreover, this type of decoration was suggested by the binding results previously obtained in our pyrazolopyrimidine series [18] in which combination of a benzyl with a 2-furyl substituent shifted affinity toward the hA_{2A} AR. In the triazolopyrazine series, this modification enhanced both hA_1 and hA_{2A} AR affinities (compare the 2-benzyl derivatives **23–26** with the relative 2-phenyl derivatives **A**, **1–2**) while reducing ability to bind the hA_3 AR. Compounds **23–25** are indeed dually potent hA_1 and hA_{2A} ligands (K_i = 2.0–13.7 nM).

Derivatives **11** and **25**, able to bind both hA_1 and hA_{2A} ARs with nanomolar affinity, and compound **10**, highly selective for the hA_{2A} subtype, were also profiled for their antagonistic properties by

Table 1

Biological activity of compounds **1–25** at human adenosine receptors.[a]

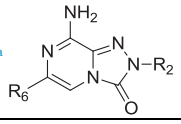

	R_6	R_2	Binding experiments K_i (nM)			cAMP assays IC_{50} (nM)
			hA_1[b]	hA_{2A}[c]	hA_3[d]	hA_{2B}[e]
1	2-furyl	Ph	13 ± 2	8.4 ± 0.9	120 ± 18	> 30,000
2	2-(5-methylfuryl)	Ph	10 ± 2.8	11 ± 1	77 ± 6.5	> 30,000
3	2-thienyl	Ph	14.1 ± 3.2	9.0 ± 2.2	42 ± 10.2	> 30,000
4	2-pyridyl	Ph	77.4 ± 5.2	13.2 ± 3.8	131.1 ± 30	> 30,000
5	C_6H_4-2-OCH_3	Ph	40.8 ± 7.1	2.0 ± 0.2	51.5 ± 3.5	> 30,000
6	C_6H_4-2-NO_2	Ph	95 ± 18	43 ± 2.4	180 ± 34	> 30,000
7	C_6H_4-3-NO_2	Ph	35.9 ± 7.8	ND[f]	38.6 ± 7.9	> 30,000
8	C_6H_4-4-NO_2	Ph	7834 ± 597	7.2 ± 1.6	16,421 ± 3505	> 30,000
9	C_6H_4-3-Br	Ph	11 ± 2	8 ± 2.1	> 30,000	> 30,000
10	C_6H_4-4-Br	Ph	> 30,000	10.6 ± 2.5	705.4 ± 139.5	> 30,000
11	C_6H_4-3-Cl	Ph	4.7 ± 1.1	6.3 ± 1	> 30,000	> 30,000
12	C_6H_4-4-Cl	Ph	14.3 ± 3.6	10.9 ± 2.7	> 30,000	> 30,000
13	C_6H_4-2-OH	Ph	16.3 ± 0.3	2.4 ± 0.5	44.5 ± 8.3	> 30,000
14	C_6H_4-2-NH_2	Ph	191 ± 28	19.5 ± 1	321 ± 63	> 30,000
15	C_6H_4-3-NH_2	Ph	15.0 ± 3.0	10.9 ± 2.3	169 ± 13.5	> 30,000
16	C_6H_4-4-NH_2	Ph	33.5 ± 6.7	22.9 ± 0.2	253.7 ± 67.6	> 30,000
17	C_6H_4-2-(piperazin-1-yl)-	Ph	1640 ± 237	1528 ± 100	4465 ± 653	> 30,000
18	C_6H_4-3-(piperazin-1-yl)-	Ph	36.1 ± 8.4	ND[f]	410.1 ± 89.2	> 30,000
19	C_6H_4-4-(piperazin-1-yl)-	Ph	265.1 ± 14.4	90.4 ± 8	1905 ± 314	> 30,000
20	C_6H_4-3-(N-dimethyl$^+$-piperazin-1-yl)-	Ph	57.1 ± 2.9	89.8 ± 2.8	3783 ± 667	> 30,000
21	C_6H_4-3-(4-benzylpiperazin-1-il)-	Ph	235.7 ± 39.9	32.3 ± 7.5	298.1 ± 49.8	> 30,000
22	C_6H_4-4-(4-benzylpiperazin-1-yl)-	Ph	121 ± 28	29 ± 1.5	> 30,000	> 30,000
23	Ph	CH_2Ph	2.4 ± 0.5	4.4 ± 0.1	223.7 ± 4.8	> 30,000
24	2-furyl	CH_2Ph	13.7 ± 0.3	2 ± 0.1	1131 ± 132	> 30,000
25	2-(5-methylfuryl)	CH_2Ph	3.7 ± 0.2	4.6 ± 1.3	112 ± 2	> 30,000
A[g]	Ph	Ph	13 ± 1	10 ± 3	11 ± 2	> 30,000

[a] Data (n = 3–5) are expressed as means ± standard errors.
[b] Displacement of specific [^{3}H]-CCPA binding at hA_1 AR expressed in CHO cells.
[c] Displacement of specific [^{3}H]-NECA binding at hA_{2A} AR expressed in CHO cells.
[d] Displacement of specific [^{3}H]-HEMADO binding at hA_3 AR expressed in CHO cells.
[e] IC_{50} values of the inhibition of NECA-stimulated adenylyl cyclase activity in CHO cells expressing hA_{2B} AR.
[f] Not determined.
[g] Ref. [21].

Table 2
Potencies of compounds **10, 11** and **25** at hA_1 and/or hA_{2A} ARs.

	hA_1 AR IC_{50} (nM)[a]	hA_{2A} AR IC_{50} (nM)[b]
10	Nd[c]	694 ± 74
11	298 ± 58	374 ± 52
25	675 ± 123	521 ± 79

[a] IC_{50} values obtained counteracting the NECA-induced decrease of cAMP accumulation in CHO cells expressing hA_1 AR.
[b] IC_{50} values obtained by inhibition of NECA-stimulated adenylyl cyclase activity in CHO cells expressing hA_{2A} AR.
[c] Not determined.

evaluating their effect on cAMP production in CHO cells, stably expressing the hA_1 and hA_{2A} ARs. The obtained results (Table 2) showed that the compounds behaved as antagonists being able to counteract NECA-inhibited (A_1) or NECA-stimulated (A_{2A}) cAMP accumulation.

Finally, we biologically evaluated also the 3,8-dione derivatives **39–53, 71–73** (Table 3) since they were thought to possess some affinity for the hA_3 subtype, given the K_i value (96 nM) of the previously reported 2,6-diphenyl-derivative **B** [21]. Actually, only three compounds (**39**, **52** and **71**) showed some hA_3 affinity (K_i = 193–274 nM), while most of them possess low (K_i = 566–7265 nM) to null affinity (K_i > 30,000 nM) for this receptor. No interesting binding data was found at the other ARs, except for compound **52**, featuring a 3-aminophenyl group at position 6, which displayed a good affinity for the hA_1 subtype (K_i = 71.3 nM).

2.4. Neuroprotection studies in SH-SY5Y cell lines

The selected compounds **10**, **11** and **25** were tested to evaluate their ability in counteracting β-amyloid peptide (Aβ)-induced toxicity. For this purpose we used the neuronal cell line SH-SY5Y (human neuroblastoma) a widely used catecholaminergic in vitro model for studies on pathologies or toxicities affecting the nervous system [16,27–29]. The 25–35 amino acid Aβ fragment was used for setting up a model of neurotoxicity [16]: it was previously incubated (at 2 and 10 μM) at 37 °C to allow peptide aggregation, days 3 and 7 were evaluated to establish the optimal time point. The obtained aggregates were incubated with cells for increasing times (24, 48 and 72 h), and subsequently cell viability was assessed via the MTT assay. Results are shown in Table 4. We chose 48 h incubation with 7 days aggregated-Aβ as the most suitable, concentration-dependent condition for screening the new compounds (cell viability of control was arbitrarily set to 100%).

Derivatives **10**, **11** and **25** (0.1–1 μM), and caffeine as reference compound, were co-incubated with SH-SY5Y cells (1×10^4 cell/well) for 48 h in the presence of Aβ 25–35 (2 and 10 μM). Fig. 2 shows the decrease of cell viability induced by 2 μM Aβ up to 73.3 ± 2.1%. Compounds **10** and **25** significantly prevented Aβ toxicity starting from concentration 0.3 μM, and **25** completely restored viability to control level. The higher concentration of Aβ 25–35 (10 μM, previously aggregated for 7 days) decreased cell vitality to 63.2 ± 4.6% (Fig. 3). Compound **10** was protective when co-incubated at 0.3 μM whereas **25** was able to significantly prevent cell mortality from 0.1 μM. In the concentration range 0.1–1 μM, both compound **11** and

Table 3

Biological activities of compounds **39–53, 71–73** at human adenosine receptors.[a]

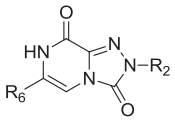

39-53, 71-73

			Binding experiments K_i (nM)			cAMP assays IC_{50} (nM)
	R_6	R_2	hA_1[b]	hA_{2A}[c]	hA_3[d]	hA_{2B}[e]
39	2-furyl	Ph	> 30,000	> 30,000	193 ± 54	> 30,000
40	2-(5-methylfuryl)	Ph	ND[f]	ND[f]	ND[f]	ND[f]
41	2-thienyl	Ph	> 30,000	> 30,000	566 ± 147	> 30,000
42	2-pyridyl	Ph	1153 ± 169	> 30,000	1047 ± 112	> 30,000
43	C_6H_4-2-OCH_3	Ph	496 ± 89	769 ± 162	7265 ± 1061	> 30,000
44	C_6H_4-2-NO_2	Ph	> 30,000	> 30,000	> 30,000	> 30,000
45	C_6H_4-3-NO_2	Ph	> 30,000	> 30,000	> 30,000	> 30,000
46	C_6H_4-4-NO_2	Ph	> 30,000	28,940 ± 990	> 30,000	> 30,000
47	C_6H_4-3-Br	Ph	> 30,000	> 30,000	> 30,000	> 30,000
48	C_6H_4-4-Br	Ph	> 30,000	> 30,000	> 30,000	> 30,000
49	C_6H_4-3-Cl	Ph	> 30,000	> 30,000	> 30,000	> 30,000
50	C_6H_4-4-Cl	Ph	> 30,000	> 30,000	> 30,000	> 30,000
51	C_6H_4-2-OH	Ph	1453 ± 352	30,810 ± 2160	1015 ± 110	> 30,000
52	C_6H_4-3-NH_2	Ph	71.3 ± 15.7	ND[f]	274.1 ± 60.7	> 30,000
53	C_6H_4-4-NH_2	Ph	552.2 ± 117.6	> 30,000	821.7 ± 180	> 30,000
71	Ph	CH_2Ph	3735 ± 690	1635.5 ± 149.5	253.7 ± 67.6	> 30,000
72	2-furyl	CH_2Ph	1456 ± 209	1421 ± 307	3184 ± 637	> 30,000
73	2-(5-methylfuryl)	CH_2Ph	> 30,000	> 30,000	1620 ± 102	> 30,000
B[g]	Ph	Ph	> 30,000	> 30,000	96 ± 15	> 30,000

[a] Data (n = 3–5) are expressed as means ± standard errors.
[b] Displacement of specific [^{3}H]-CCPA binding at hA_1 AR expressed in CHO cells.
[c] Displacement of specific [^{3}H]-NECA binding at hA_{2A} AR expressed in CHO cells.
[d] Displacement of specific [^{3}H]-HEMADO binding at hA_3 AR expressed in CHO cells.
[e] IC_{50} values of the inhibition of NECA-stimulated adenylyl cyclase activity in CHO cells expressing hA_{2B} AR.
[f] Not determined.
[g] Ref. [21].

caffeine were ineffective. Derivatives **10**, **11** and **25**, as well as caffeine, did not alter cell viability *per se* when tested in the absence of Aβ (data not shown).

To summarize, **11** did not exhibit a protective effect on cell viability, nor did caffeine, while **10** and **25** were active against the neurotoxicity evoked by incubating neuronal cells with Aβ aggregates. Thus, derivatives **11** and **25**, although showing similar nanomolar hA_1 and hA_{2A} AR affinities, exerted a significantly different effect on cell viability at the tested concentrations probably due to differences between the binding experiment model and the cellular model or to other compound properties. In any case, the results obtained in these experiments highlight the potential of our triazolopyrazine derivatives as new possible neuroprotective agents in AD.

2.5. Molecular modeling studies

Molecular docking analyses were performed to simulate the binding mode of the synthesized compounds at the hA_{2A} AR cavity. As molecular target, we chose the high-resolution crystal structure of the hA_{2A} AR in complex with the antagonist/inverse agonist ZM241385 (http://www.rcsb.org; pdb code: 5NM4; 1.7-Å resolution [30]). MOE (Molecular Operating Environment 2014.09 [31]) docking tool ("induced fit"

Table 4
Toxic effect induced by β-amyloid protein (Aβ fragment 25–35 aa).[a]

Time of incubation with cells		Cell viability %	Time of preventive aggregation of Aβ 25–35	
24 h			3 days	7 days
	Control	100 ± 4.2		
	Aβ 25–35, 2 μM		92.8 ± 1.9	69.6 ± 2.9**
	Aβ 25–35, 10 μM		80.3 ± 4.5*	64.4 ± 3.8**
48 h			3 days	7 days
	Control	100 ± 7.2		
	Aβ 25–35, 2 μM		80.5 ± 7.6	73.3 ± 2.1*
	Aβ 25–35, 10 μM		69.8 ± 5.4**	63.2 ± 4.6**
72 h			3 days	7 days
	Control	100 ± 8.9		
	Aβ 25–35, 2 μM		95.5 ± 15.1	108.1 ± 16.3
	Aβ 25–35, 10 μM		83.0 ± 11.4	68.7 ± 8.7**

[a] Aggregation of β-amyloid peptide (Aβ fragment 25–35 aa; 2 and 10 μM) was allowed for 3 and 7 days at 37 °C. The so obtained different proteins aggregates were tested in SH-SY5Y cell (1×10^4 cell/well) to evaluate the cytotoxic effect. Incubation was performed for increasing times (24, 48 and 72 h), subsequently cell viability was assessed via the MTT assay. Viability is expressed as % in comparison to the control cells (arbitrarily set 100% of viable cells). Data are presented as mean ± SEM of 3 different experiments performed in quintuplicate. One-way ANOVA with a Bonferroni post-hoc test was used to compare different treatments. *$P < 0.05$ and **$P < 0.01$ versus control.

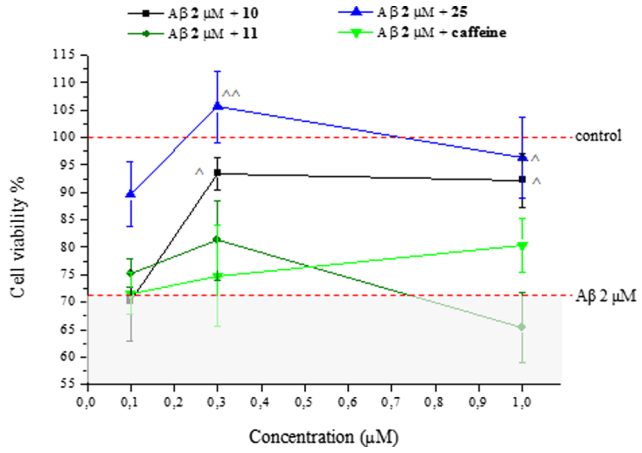

Fig. 2. SH-SY5Y cell (1×10^4 cell/well) were incubated 48 h with compounds **10**, **11** and **25** (0.1, 0.3 and 1 μM) in the presence of β-amyloid peptide (Aβ fragment 25–35 aa; 2 μM following 7 days of 37 °C aggregation). Caffeine was used as reference compound. Cell vitality was assessed via MTT assay. Viability is expressed as % in comparison to the control cells (arbitrarily set 100% of viable cells). Dashed lines represent values of control and Aβ-treated samples. Data are presented as mean ± SEM of 3 different experiments performed in quintuplicate. One-way ANOVA with a Bonferroni post-hoc test was used to compare different treatments. ^P < 0.05 and ^^P < 0.01 versus β-amyloid effect.

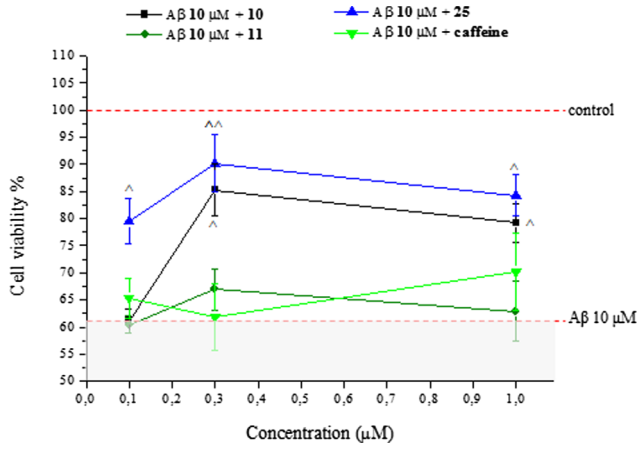

Fig. 3. SH-SY5Y cell (1×10^4 cell/well) were incubated 48 h with compounds **10**, **11** and **25** (0.1, 0.3 and 3 μM) in the presence of β-amyloid peptide (Aβ fragment 25–35 aa; 10 μM following 7 days of 37 °C aggregation). Caffeine was used as reference compound. Cell vitality was assessed via MTT assay. Viability is expressed as % in comparison to the control cells (arbitrarily set 100% of viable cells). Dashed lines represent values of control and Aβ-treated samples. Data are presented as mean ± SEM of 3 different experiments performed in quintuplicate. One-way ANOVA with a Bonferroni post-hoc test was used to compare different treatments. ^P < 0.05 and ^^P < 0.01 versus β-amyloid effect.

setting) and Gold [32] and Autodock software [33,34] were employed for this task. Analogously to a previous study at the same receptor [21], we performed docking analyses with various docking tools to get a sort of average binding mode prediction of the compounds at the hA_{2A} AR binding cavity.

The docking results show that the molecules could bind to the receptor binding pocket with a preferred arrangement already observed for analogue compounds at the same receptor [21]. In this arrangement (named "type-one" conformation in the previous study), the compounds present the substituent at the 2-position (R_2) located in the depth of the cavity and the R_6 group at the entrance of the binding site (Fig. 4A and B), with the triazolopyrazinone scaffold being able to interact with

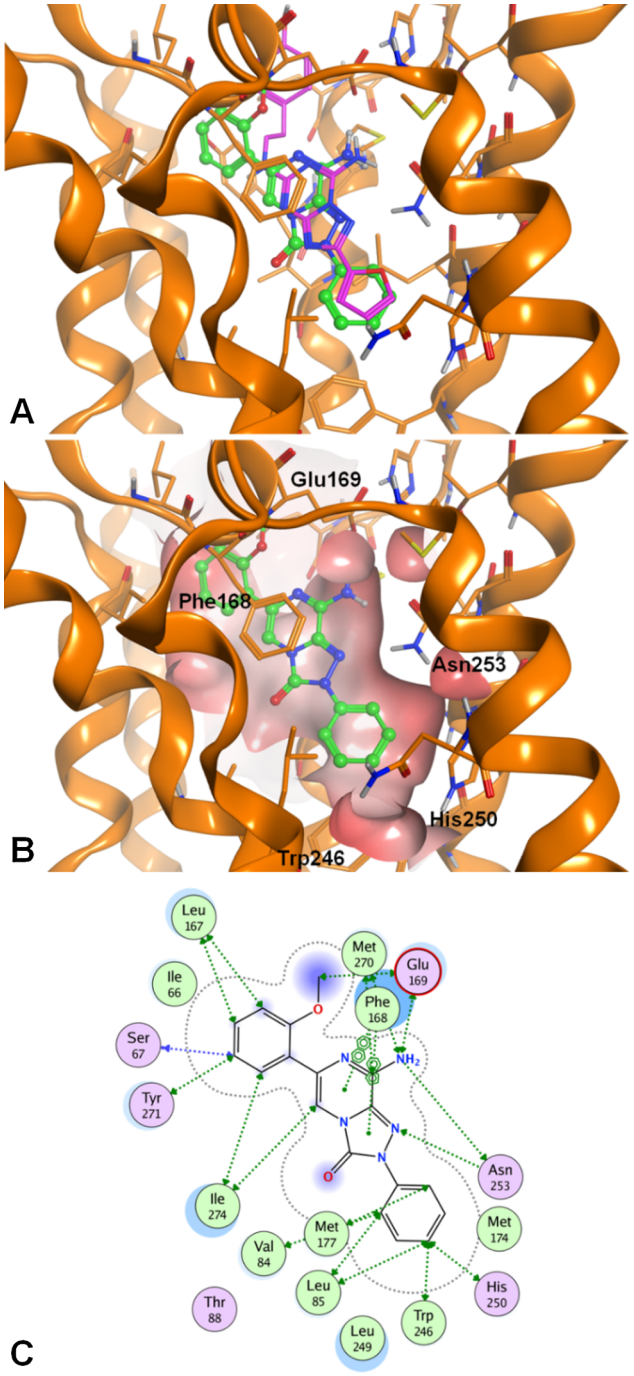

Fig. 4. (A and B) The type-one docking conformation of the synthesized compounds at the hA_{2A} AR cavity, representing the preferred binding mode according to docking-scoring results; compound **5** (green) is represented superimposed to the co-crystallized reference hA_{2A} AR inverse agonist ZM241385 (magenta, panel A) and alone within the receptor cavity (panel B), with key receptor residues indicated. (C) Schematic description of the ligand-target interaction (built within MOE software).

Asn253$^{6.55}$ and Glu169 (EL2) through H-bond contacts and with the phenyl ring of Phe168 (EL2) through a π-π interaction (Fig. 4C). This interaction is very similar also to the one observed for the co-crystallized compound ZM241,385 at the hA_{2A} AR (Fig. 4A) [30]. An alternative binding mode ("type-two" conformation, generally associated to lower docking scores) makes the compounds be oriented in an opposite way, with the R_2 and R_6 groups located at the entrance and in the depth of the binding cavity, respectively.

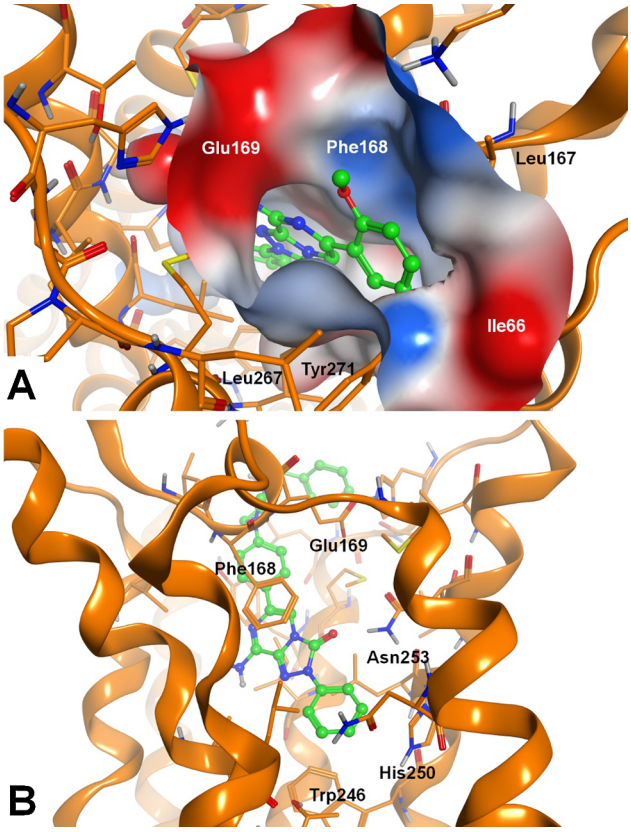

Fig. 5. (A) Top view of the type-one docking conformation of compound **5** at the hA_{2A} AR; the key residues for the interaction with 6-substituent are indicated and the cavity entrance is represented as molecular surface, with red-to-blue regions indicating negatively-to-positively charged regions, respectively. (B) Alternative binding mode of the synthesized compounds presenting a large substituent in the para-position of the 6-phenyl ring (compound **22** is shown). The key ligand-target polar interaction is between the 3-carbonyl group of the compound and the $Asn253^{6.55}$ amide function.

Compound **A** is a sort of prototype of the series, as it presents two unsubstituted phenyl rings at the 2- and 6- positions. This molecule possesses high affinities for the hA_1, hA_{2A} and hA_3 ARs and this makes compound **A** a sort of *passe-partout* for the three ARs. Docking results of this derivative at the structures of the ARs [21] showed that it may be inserted in the cavities with both binding modes associated to good docking scores (the "type-one" generally awarded with better values). The possibility of making various complexes with the same receptor could lead to good affinity data at this protein and this factor could be applied at the three ARs.

Docking results for derivatives **5–22** show that these molecules bind the hA_{2A} AR cavity almost exclusively with the type-one docking arrangement. The substituents inserted on the 6-phenyl ring appear to modulate the affinity for the three AR subtypes. The compounds featuring a small ortho-substituent (**5**, **13**, **14**) are generally endowed with low nanomolar hA_{2A} AR affinity. This substituent is oriented toward the N7 atom and in proximity of the Glu169 (EL2) residue, with a possibility of giving polar interaction with the nitrogen atom of the compound scaffold or with the backbone or sidechain atoms of the above cited receptor residue (Fig. 5A). Introduction of a nitro group at the ortho position of the 6-phenyl ring (**6**) affords a lower hA_{2A} AR affinity, mainly due to higher hindrance of the substituent and consequent lower ability of the compound to maintain the co-planarity of the 6-phenyl ring with the heterocyclic scaffold. An electronic repulsion with the Glu169 (EL2) side chain is an additional factor at the basis of the lower affinity of this compound. Introduction of an even bigger ortho-substituent, like a piperazinyl group (**17**), leads to a drop in the hA_{2A} AR affinity.

Compounds presenting a substituent at the meta or para position of the 6-phenyl ring (**7–12**, **15**, **16**, **19–22**) are endowed with low nanomolar affinity. Even these compounds appear to exclusively bind to the hA_{2A} AR with the type-one docking conformation. This is evident for compounds bearing small substituents on the 6-phenyl ring. These groups get located in proximity of H-bond donor functions of the receptor, such as the backbone NH groups of Phe168 and Glu169 (EL2) and the hydroxyl group of $Tyr271^{7.36}$. Even the side chains of (EL2) and Leu267 (EL3) are in proximity to these compound substituents, allowing non-polar interaction. Compounds bearing large substituents at the meta position of the 6-phenyl ring (**20**, **21**) adopt the type-one docking conformation as well. The compounds featuring a large substituent at the para position of the same ring (**19**, **22**) are inserted in the binding pocket with an upside-down conformation, where the 2-phenyl ring is inserted in the depth of the cavity while the scaffold is oppositely oriented with the 3-carbonyl group pointing toward the $Asn253^{6.55}$ amide function (Fig. 5B).

Compounds bearing a heterocyclic moiety at the 6-position and a phenyl ring at the 2-position (**1–4**) may adopt both type-one and type-two docking conformations, like compound **A**, with a fair preference for the type-two conformation (the one pointing the 2-phenyl ring toward the extracellular environment). This behaviour may explain the high affinity of these derivatives for the hA_{2A} AR binding cavity, analogously to the reference compound (**A**). When the 2-phenyl ring is replaced by a benzyl moiety and a heterocyclic ring is inserted at the 6-position (**23–25**), the compounds preferentially adopt a type-two docking conformation, pointing the 2-substituent toward the extracellular environment. For both these sets (**1–4** and **23–25**) the steric and chemical-physical profile of the 6-substituent modulates the hA_{2A} AR affinity, with the 2-furyl providing the highest affinity data within each set, as expected.

Docking experiments at a hA_1 AR crystal structure (pdb code: 5UEN; 3.2-Å resolution [35]) were also simulated with the same docking tools and protocols as above. Even for this receptor, we observed two families of conformations, where the preference of the compounds for a specific arrangement (type-one or type-two binding mode) appears in accordance with that observed from docking studies at the hA_{2A} AR (see above). As previously noted for analogue triazolopyrazinone-based compounds [21], some residues at the entrance of the hA_1 AR binding cavity (Glu170, Ser267, and $Tyr271^{7.36}$) and in proximity to the 6-substituents (type-one conformations) are different in some cases with respect to the corresponding ones in the hA_{2A} AR (Leu167, Leu267, and $Tyr271^{7.36}$), leading to a slightly different interaction with the compounds with respect to the hA_{2A} AR subtype [21]. Nevertheless, the interactions between these molecules and the hA_{2A} AR and hA_1 AR are generally conserved, leading to similar affinity data for several derivatives at these two AR subtypes.

3. Conclusion

In this work, an enlarged set of 1,2,4-triazolo[4,3-*a*]pyrazine-3-one derivatives was synthesized to deepen SAR studies and to obtain hA_{2A} AR selective antagonists or dual-targeting hA_1 and hA_{2A} AR antagonists which were of our interest for their potential neuroprotective effect. The aim of the work can be considered satisfied. In fact, compounds **8** and **10**, featuring a 2-phenyl ring and, respectively, a 4-nitro and 4-bromo substituent on the 6-phenyl moiety, showed high hA_{2A} AR affinity (K_i = 7.2 and 10.6 nM) and a complete selectivity for this AR subtype. Several derivatives possessed nanomolar affinity (K_i < 20 nM) for both hA_1 and hA_{2A} ARs and different degrees of selectivity versus the hA_3 AR. Results of docking studies at the hA_{2A} and hA_1 AR crystal structures have been helpful to rationalize the observed affinity data and to highlight that the steric hindrance of the substituents at the 2- and 6-position of the bicyclic core affects the compound arrangement in the receptor binding cavity.

Among the selected compounds **10**, **11** and **25**, tested to evaluate their neuroprotective effect in an in vitro AD model, the 2-phenyl-6-(4-

bromophenyl) derivative **10** and the 2-benzyl-6-(5-methyl-2-furanyl) derivative **25** were able to counteract the Aβ-induced toxicity in cultured human neuroblastoma SH-SY5Y cells. Due to these interesting behaviors, further investigations are in progress on the 1,2,4-triazolo [4,3-*a*]pyrazines series to develop new derivatives as neuroprotective agents.

4. Experimental

4.1. Chemistry

The microwave-assisted syntheses were performed using an Initiator EXP Microwave Biotage instrument (frequency of irradiation: 2.45 GHz). Silica gel 60 (Merck, 70–230 mesh) was used for analytical TLC, and for column chromatography, respectively. All melting points were determined on a Gallenkamp melting point apparatus and are uncorrected. Elemental analyses were performed with a Flash E1112 Thermofinnigan elemental analyzer for C, H, N and the results were within 0.4% of the theoretical values. All final compounds revealed purity not less than 95%. The IR spectra were recorded with a Perkin-Elmer Spectrum RX I spectrometer in Nujol mulls and are expressed in cm^{-1}. NMR spectra were recorded on a Bruker Avance 400 spectrometer (400 MHz). The chemical shifts are reported in δ (ppm) and are relative to the central peak of the solvent which was $CDCl_3$ or $DMSOd_6$. The following abbreviations are used: s = singlet, d = doublet, t = triplet, q = quartet, m = multiplet, br = broad and ar = aromatic protons.

4.1.1. General procedure for the synthesis of ethyl 4-(2-aryl/heteroaryl-2-oxoethyl)-5-oxo-1-phenyl-4,5-dihydro-1H-1,2,4-triazole-3-carboxylate derivatives **27–38**.

The suitable α-bromoketone (1.2 mmol), all commercially available except the heteroaryl derivatives [36–39], was added to a mixture of ethyl 1-phenyl-5-oxo-1,2,4-triazole-3-carboxylate derivative **26** [21] (1 mmol) and K_2CO_3 (2 mmol) in DMF/CH_3CN (1:9, 10 mL). The suspension was stirred at room temperature until the disappearance of the starting material (TLC monitoring, 2–24 h). The solvent was removed at reduced pressure and the residue was treated with water (50–70 mL). The resulting precipitate was collected by filtration, washed with water (20 mL), Et_2O (10 mL) and then recrystallized.

4.1.1.1. Ethyl 4-[2-(furan-2-yl)-2-oxoethyl]-5-oxo-1-phenyl-4,5-dihydro-1H-1,2,4-triazole-3-carboxylate ***(27)***. Yield 72%; m.p. 170–172 °C (EtOH). ^{1}H NMR (DMSO-d_6) 1.22 (t, 3H, CH_3, J = 7.1 Hz), 4.31 (q, 2H, CH_2, J = 7.1 Hz), 5.37 (s, 2H, CH_2), 6.84 (d, 1H, furan proton, J = 2.0 Hz),7.35–7.38 (m, 1H, ar), 7.53–7.57 (m, 2H, ar),7.75 (d, 1H, furan proton, J = 2.0 Hz), 7.93 (d, 2H, ar, J = 7.4 Hz), 8.15 (m, 1H, furan proton).

4.1.1.2. Ethyl 4-[2-(5-methylfuran-2-yl)-2-oxoethyl]-5-oxo-1-phenyl-4,5-dihydro-1H-1,2,4-triazole-3-carboxylate ***(28)***. Yield 58%; m.p. 142–144 °C (Cyclohexane/AcOEt). ^{1}H NMR ($CDCl_3$) 1.40 (t, 3H, CH_3, J = 7.1 Hz), 2.46 (s, 3H, CH_3), 4.42 (q, 2H, CH_2, J = 7.1 Hz), 5.40 (s, 2H, CH_2), 6.26 (d, 1H, furan proton, J = 2.8 Hz), 7.31–7.33 (m, 2H, 1 ar, 1 furan proton), 7.47 (t, 2H, ar, J = 7.7 Hz), 8.03 (d, 2H, ar, J = 8.4 Hz).

4.1.1.3. Ethyl 4-[2-(thiophen-2-yl)-2-oxoethyl]-5-oxo-1-phenyl-4,5-dihydro-1H-1,2,4-triazole-3-carboxylate ***(29)***. Yield 80%; m.p. 167–168 °C (EtOH). ^{1}H NMR (DMSO-d_6) 1.21 (t, 3H, CH_3, J = 7.1 Hz), 4.31 (q, 2H, CH_2, J = 7.1 Hz), 5.52 (s, 2H, CH_2), 7.35–7.39 (m, 2H, CH_2), 7.55 (t, 2H, ar, J = 7.8 Hz), 7.94 (d, 2H, ar, J = 7.7 Hz), 8.18 (d, 1H, ar, J = 4.0 Hz), 8.28 (d, 1H, ar, J = 2.9 Hz).

4.1.1.4. Ethyl 4-[2-(pyrid-2-yl)-2-oxoethyl]-5-oxo-1-phenyl-4,5-dihydro-1H-1,2,4-triazole-3-carboxylate ***(30)***. Yield 30%; m.p. 153–155 °C (EtOH). ^{1}H NMR (DMSO-d_6) 1.29 (t, 3H, CH_3, J = 7.0 Hz), 4.29 (q, 2H, CH_2, J = 7.0 Hz), 5.67 (s, 2H, CH_2), 7.37 (t, 1H, ar, J = 7.4 Hz), 7.55 (t, 2H, ar, J = 7.8 Hz), 7.80 (t, 1H, ar, J = 3.1 Hz), 7.82 (d, 1H, ar, J = 4.8 Hz), 7.95 (d, 1H, ar, J = 8.5 Hz), 8.05 (d, 1H, ar, J = 7.8 Hz), 8.11 (t, 1H, ar, J = 7.7 Hz), 8.85 (d, 1H, ar, J = 4.7 Hz).

4.1.1.5. Ethyl 4-[2-(2-methoxyphenyl)-2-oxoethyl]-5-oxo-1-phenyl-4,5-dihydro-1H-1,2,4-triazole-3-carboxylate ***(31)***. Yield 53%; m.p. 155–157 °C (EtOH). ^{1}H NMR (DMSO-d_6) 1.21 (t, 3H, CH_3, J = 7.1 Hz), 4.02 (q, 2H, CH_2, J = 7.1 Hz), 4.31 (s, 3H, OCH_3), 5.37 (s, 2H, CH_2), 7.12 (t, 1H, ar, J = 7.5 Hz), 7.30 (d, 1H, ar, J = 8.6 Hz), 7.36 (t, 1H, ar, J = 7.4 Hz), 7.55 (t, 2H, ar, J = 7.6 Hz), 7.70 (t, 1H, ar, J = 7.8 Hz), 7.79 (d, 1H, ar, J = 7.8 Hz), 7.90 (d, 2H, ar, 7.9 Hz).

4.1.1.6. Ethyl 4-[2-(2-nitrophenyl)-2-oxoethyl]-5-oxo-1-phenyl-4,5-dihydro-1H-1,2,4-triazole-3-carboxylate ***(32)***. Yield 92%; m.p. 171–173 °C (EtOH). ^{1}H NMR ($CDCl_3$) 1.49 (t, 3H, CH_3, J = 7.1 Hz), 4.52 (q, 2H, CH_2, J = 7.1 Hz), 5.44 (s, 2H, CH_2), 7.32 (t, 1H, ar, J = 7.4 Hz), 7.48 (t, 2H, ar, J = 7.8 Hz), 7.70–7.77 (m, 2H, ar), 7.84 (t, 1H, ar, J = 7.3 Hz), 8.04 (d, 2H, ar, J = 7.9 Hz), 8.22 (d, 1H, ar, J = 8.2 Hz).

4.1.1.7. Ethyl 4-[2-(3-nitrophenyl)-2-oxoethyl]-5-oxo-1-phenyl-4,5-dihydro-1H-1,2,4-triazole-3-carboxylate ***(33)***. Yield 89%; m.p. 134–136 °C (Cyclohexane/EtOAc). ^{1}H NMR (DMSO-d_6) 1.20 (t, 3H, CH_3, J = 7.1 Hz), 4.30 (q, 2H, CH_2, J = 7.3 Hz), 5.71 (s, 2H, CH_2), 7.39 (t, 1H, ar, J = 7.4 Hz), 7.56 (t, 2H, ar, J = 8.1 Hz), 7.91–7.95 (m, 3H, ar), 8.57 (t, 2H, ar, J = 8. 6 Hz), 8.78 (s, 1H, ar).

4.1.1.8. Ethyl-4-[2-(4-nitrophenyl)-2-oxoethyl]-5-oxo-1-phenyl-4,5-dihydro-1H-1,2,4-triazole-3-carboxylate ***(34)***. Yield 97%; m.p. 180–182 °C (EtOH/CH_3NO_2). ^{1}H NMR (DMSO-d_6) 1.21 (t, 3H, CH_3, J = 7.1 Hz), 4.30 (q, 2H, CH_2, J = 7.1 Hz), 5.67 (s, 2H, CH_2), 7.37 (t, 1H, ar, J = 7.5 Hz), 7.56 (t, 2H, ar, J = 8.3 Hz), 7.94 (d, 2H, ar, J = 7.8 Hz), 8.35 (d, 2H, ar, J = 8.8 Hz), 8.43 (d, 2H, ar, J = 8.8 Hz).

4.1.1.9. Ethyl 4-[2-(3-bromophenyl)-2-oxoethyl]-5-oxo-1-phenyl-4,5-dihydro-1H-1,2,4-triazole-3-carboxylate ***(35)***. Yield 62%; m.p. 200–202 °C (EtOH). ^{1}H NMR ($CDCl_3$) 1.40 (t, 3H, CH_3, J = 7.1 Hz), 4.42 (q, 2H, CH_2, J = 7.1 Hz), 5.54 (s, 2H, CH_2), 7.32 (t, 1H, ar, J = 7.5 Hz), 7.43–7.5 (m, 3H, ar), 7.81 (d, 1H, ar, J = 8 Hz), 7.96 (d, 1H, ar, J = 7.8 Hz), 8.02 (d, 2H, ar, J = 8.2 Hz), 8.16 (t, 1H, ar, J = 1.8 Hz).

4.1.1.10. Ethyl 4-[2-(4-bromophenyl)-2-oxoethyl]-ethyl-5-oxo-1-phenyl-4,5-dihydro-1H-1,2,4-triazole-3-carboxylate ***(36)***. Yield 77%; m.p. 167–169 °C (EtOH). ^{1}H NMR ($CDCl_3$) 1.39 (t, 3H, CH_3, J = 7.1 Hz), 4.42 (q, 2H, CH_2, J = 7.1 Hz), 5.53 (s, 2H, CH_2), 7.32 (t, 1H, ar, J = 7.5 Hz), 7.48 (t, 2H, ar, J = 8.4 Hz), 7.71 (d, 2H, ar, J = 6.7 Hz), 7.90 (d, 2H, ar, J = 8.6 Hz), 8.02 (d, 2H, ar, J = 7.8 Hz).

4.1.1.11. Ethyl 4-[2-(3-chlorophenyl)-2-oxoethyl]-5-oxo-1-phenyl-4,5-dihydro-1H-1,2,4-triazole-3-carboxylate ***(37)***. Yield 47%; m.p. 141–143 °C (EtOH). ^{1}H NMR (DMSO-d_6) 1.20 (t, 3H, CH_3, J = 7.1 Hz), 4.30 (q, 2H, CH_2, J = 7.1 Hz), 5.61 (s, 2H, CH_2), 7.37 (t, 1H, ar, J = 7.6 Hz), 7.56 (t, 2H, ar, J = 7.6 Hz), 7.67 (t, 1H, ar, J = 7.9 Hz), 7.83–7.85 (dd, 1H, ar, J = 1.2 Hz, J = 6.7 Hz), 7.94 (d, 2H, ar, J = 7.7 Hz), 8.08 (d, 1H, ar, J = 7. 8 Hz), 8.14 (t, 1H, ar, J = 1.8 Hz).

4.1.1.12. Ethyl 4-[2-(4-chlorophenyl)-2-oxoethyl]-ethyl-5-oxo-1-phenyl-4,5-dihydro-1H-1,2,4-triazole-3-carboxylate ***(38)***. Yield 60%; m.p. 194–196 °C (MeOH). ^{1}H NMR (DMSO-d_6) 1.20 (t, 3H, CH_3, J = 7.1 Hz), 4.30 (q, 2H, CH_2, J = 7.1 Hz), 5.59 (s, 2H, CH_2), 7.37 (t, 1H, ar, J = 7. 4 Hz), 7.55 (t, 2H, ar, J = 7.5 Hz), 7.70 (d, 2H, ar, J = 8.6 Hz), 7.94 (d, 2H, ar, J = 7.9 Hz), 8.13 (d, 2H, ar, J = 8.7 Hz).

*4.1.2. General procedure for the synthesis of 2-phenyl-1,2,4-triazolo[4,3-a] pyrazine-3,8(2H,7H)-dione derivatives **39–50***

A mixture of the suitable ethyl 1,2,4-triazole-3-carboxylate derivatives **27–38** (0.9 mmol) and anhydrous ammonium acetate (3.5 mmol) was heated in a sealed tube at 150 °C until the disappearance of starting material (TLC monitoring, 3–24 h). The residue was taken up with EtOH (1 mL) and Et_2O (5 mL), collected by filtration and washed with water (20 mL). All the crude compounds were purified by recrystallization.

*4.1.2.1. 6-(2-Furan-2-yl)-2-phenyl-1,2,4-triazolo[4,3-a]pyrazine-3,8(2H,7H)-dione (**39**)*. Yield 73%; m.p. 298–299 °C (EtOH). ^{1}H NMR (DMSO-d_6) 6.65–6.67 (m, 1H, furan proton), 7.16 (s, 1H, H-5), 7.21 (d, 1H, furan proton, J = 1.8 Hz),7.35–7.38 (m, 1H, ar), 7.54–7.58 (m, 2H, ar), 7.80–7.82 (m, 1H, furan proton), 7.99–8.01 (m, 2H, ar), 11.71 (br s, 1H, NH). IR 3187, 3123, 1691.

*4.1.2.2. 2-Phenyl-6-(5-methylfuran-2-yl)-1,2,4-triazolo[4,3-a]pyrazine-3,8(2H,7H)-dione (**40**)*. Yield 75%; m.p. 281–283 °C (AcOH). ^{1}H NMR (DMSO-d_6) 2.35 (s, 3H, CH_3), 6.26 (d, 1H, furan proton, J = 2.3 Hz), 7.07–7.08 (m, 2H, H-5 + furan proton), 7.36 (t, 1H, ar, J = 7.5 Hz), 7.56 (t, 2H, ar, J = 7.7 Hz), 8.00 (d, 2H, ar, J = 7.6 Hz) 11.63 (br s, 1H, NH).

*4.1.2.3. 2-Phenyl-6-(2-thienyl)-1,2,4-triazolo[4,3-a]pyrazine-3,8(2H,7H)-dione (**41**)*. Yield 55%; m.p. > 300 °C (2-Methoxyethanol). ^{1}H NMR (DMSO-d_6) 7.17 (q, 2H, ar, J = 3.6 Hz), 7.36 (t, 1H, ar, J = 7.4 Hz), 7.56 (t, 2H, ar, J = 7.9 Hz), 7.67 (d, 2H, ar + H-5, J = 4.4 Hz), 8.00 (d, 2H, ar, J = 7.9 Hz), 11.70 (br s, 1H, NH).

*4.1.2.4. 2-Phenyl-6-(2-pyridyl)-1,2,4-triazolo[4,3-a]pyrazine-3,8(2H,7H)-dione (**42**)*. Yield 70%; m.p. 264–265 °C (EtOH/2-Methoxyethanol). ^{1}H NMR (DMSO-d_6) 7.38 (t, 1H, ar, J = 7.4 Hz), 7.46 (t, 1H, ar, J = 4.1 Hz), 7.57 (t, 2H, ar, J = 8.0 Hz), 7.92–7.97 (m, 2H, ar + H-5), 8.02 (d, 2H, ar, J = 8.4 Hz), 8.19 (d, 1H, ar, J = 8.1 Hz), 8.68 (d, 1H, pyridine proton, J = 4.8 Hz), 11.02 (br s, 1H, NH). IR 3254, 1688.

*4.1.2.5. 6-(2-Methoxyphenyl)-2-phenyl-1,2,4-triazolo[4,3-a]pyrazine-3,8(2H,7H)-dione (**43**)*. Yield 77%; m.p. 279–281 °C (2-Methoxyethanol/DMF). ^{1}H NMR (DMSO-d_6) 3.84 (s, 3H, CH_3), 7.02 (s, 1H, H-5), 7.05 (t, 1H, ar, J = 8.3 Hz), 7.15 (d, 1H, ar, J = 8.0 Hz), 7.36 (t, 1H, ar, J = 7.4 Hz), 7.41–7.49 (m, 2H, ar), 7.56 (t, 2H, ar, J = 8.4 Hz), 8.01 (d, 2H, ar, J = 7.6 Hz) 11.39 (br s, 1H, NH).

*4.1.2.6. 6-(2-Nitrophenyl)-2-phenyl-1,2,4-triazolo[4,3-a]pyrazine-3,8(2H,7H)-dione (**44**)*. Yield 66%; m.p. > 300 °C (2-Methoxyethanol). ^{1}H NMR (DMSO-d_6), 7.20 (s, 1H, H-5), 7.41 (t, 1H, ar, J = 7.4 Hz), 7.60 (t, 2H, ar, J = 7.6 Hz), 7.75 (d, 1H, ar, J = 6.1 Hz), 7.84 (t, 1H, ar, J = 7.6 Hz), 7. 93 (t, 1H, ar, J = 7.5 Hz), 8.02 (d, 2H, ar, J = 8.5 Hz), 8.31 (d, 1H, ar, J = 8.1 Hz), 11.8 (br s, 1H, NH).

*4.1.2.7. 6-(3-Nitrophenyl)-2-phenyl-1,2,4-triazolo[4,3-a]pyrazine-3,8(2H,7H)-dione (**45**)*. Yield 62%; m.p. > 300 °C (AcOH). ^{1}H NMR (DMSO-d_6), 7.37 (t, 1H, ar, J = 7.4 Hz), 7.55–7.59 (m, 3H, 2 ar, H-5), 7.77 (t, 1H, ar, J = 8. 0 Hz), 8.02 (d, 2H, ar, J = 7.8 Hz), 8.19 (d, 1H, ar, J = 7.7 Hz), 8.29 (d, 1H, ar, J = 8.2 Hz) 8.57 (s, 1H, ar) 11. 87 (br s, 1H, NH).

*4.1.2.8. 6-(4-Nitrophenyl)-2-phenyl-1,2,4-triazolo[4,3-a]pyrazine-3,8(2H,7H)-dione (**46**)*. Yield 88%; m.p. > 300 °C (2-Methoxyethanol/DMF). ^{1}H NMR (DMSO-d_6) 7.37 (t, 1H, ar, J = 7.4 Hz), 7.57 (m, 3H, 2 ar, H-5), 8.00–8.03 (m, 4H, ar), 8.29 (d, 2H, ar, J = 8.7 Hz), 11.83 (br s, 1H, NH).

*4.1.2.9. 6-(3-Bromophenyl)-2-phenyl-1,2,4-triazolo[4,3-a]pyrazine-3,8(2H,7H)-dione (**47**)*. Yield 47%; m.p. > 300 °C (2-Methoxyethanol). ^{1}H NMR (DMSO-d_6) 7.37 (t, 1H, ar, J = 7.4 Hz), 7.41–7.45 (m, 2H, 1 ar, H-5), 7.56 (t, 2H, ar, J = 8.4 Hz), 7.64 (d, 1H, ar, J = 8.0 Hz), 7.74 (d, 1H, ar, J = 8.6 Hz), 7.96 (s, 1H, ar), 8.02 (d, 2H, ar, J = 8.8 Hz), 11.67 (br s, 1H, NH).

*4.1.2.10. 6-(4-Bromophenyl)-2-phenyl-1,2,4-triazolo[4,3-a]pyrazine-3,8(2H,7H)-dione (**48**)*. Yield 49%; m.p. > 300 °C (AcOH/DMF). ^{1}H NMR (DMSO-d_6) 7.35–7.38 (m, 2H, 1 ar, H-5), 7.56 (t, 2H, ar, J = 7.7 Hz), 7.67 (s, 4H, ar), 8.01 (d, 2H, ar, J = 7.7 Hz), 11.62 (br s, 1H, ar).

*4.1.2.11. 6-(3-Chlorophenyl)-2-phenyl-1,2,4-triazolo[4,3-a]pyrazine-3,8(2H,7H)-dione (**49**)*. Yield 76%; m.p. > 300 °C (2-Methoxyethanol). ^{1}H NMR (DMSO-d_6) 7.37 (t, 1H, ar, J = 7.3 Hz), 7.44 (s, 1H, H-5), 7.50–7.54 (m, 2H, ar), 7.56 (t, 2H, ar, J = 7.8 Hz), 7.69–7.71 (m, 1H, ar), 7.83 (s, 1H, ar), 8.01 (d, 2H, ar, J = 7.8 Hz) 11.65 (br s, 1H, NH).

*4.1.2.12. 6-(4-Chlorophenyl)-2-phenyl-1,2,4-triazolo[4,3-a]pyrazine-3,8(2H,7H)-dione (**50**)*. Yield 81%; m.p. > 300 °C (2-Methoxyethanol/DMF). ^{1}H NMR (DMSO-d_6) 7.35–7.38 (m, 2H, 1 ar, H-5), 7.53–7.58 (m, 4H, ar), 7.74 (d, 2H, ar, J = 8.6 Hz), 8.01 (d, 2H, ar, J = 8.0 Hz), 11.66 (br s, 1H, ar). ^{13}C NMR (DMSO-d_6) 100.92, 119.58, 126.98, 127.27, 128.77, 129.22, 129.81, 130.31, 134.37, 135.96, 137.67, 147.67, 153.47.

*4.1.3. 6-(2-Hydroxyphenyl)-2-phenyl-1,2,4-triazolo[4,3-a]pyrazine-3,8(2H,7H)-dione (**51**)*.

1 M solution of BBr_3 in dichloromethane (5.1 mL) was slowly added at 0 °C, under nitrogen atmosphere, to a suspension of the methoxy derivative **43** (1.0 mmol) in anhydrous dichloromethane (20 mL). The mixture was stirred at room temperature for 18 h, then it was diluted with water (10 mL) and neutralized with a $NaHCO_3$ saturated solution. The organic solvent was removed by evaporation at reduced pressure and the solid was collected by filtration. The crude derivative was dried and purified by recrystallization. Yield 96%; m.p. > 300 °C (2-Methoxyethanol). ^{1}H NMR (DMSO-d_6) 6.90 (t, 1H, ar, J = 7.4 Hz), 6.97 (d, 1H, ar, J = 8.1 Hz), 7.13 (s, 1H, H-5), 7.28 (t, 1H, ar, J = 7.2 Hz), 7.34–7.42 (m, 2H, ar), 7.56 (t, 2H, ar, J = 7.8 Hz), 8.02 (d, 2H, ar, J = 7.9 Hz) 10.14 (br s, 1H, OH), 11.37 (br s, 1H, NH).

*4.1.4. General procedure for the synthesis of amino-substituted 1,2,4-triazolo[4,3-a]pyrazine-3,8(2H,7H)-dione derivatives **52** and **53**.*

10% Pd/C (10% w/w with respect to the nitro derivative) was added to a solution of the 6-nitrophenyl derivative **45** or **46** (1.2 mmol) in DMF (10 mL). The mixture was hydrogenated in a Parr apparatus at 40 psi for 24 h. Then the catalyst was filtered off and the clear solution was diluted with water (about 50 mL). The resulting solid was collected by filtration, washed with water and Et_2O, dried and recrystallized.

*4.1.4.1. 6-(3-Aminophenyl)-2-phenyl-1,2,4-triazolo[4,3-a]pyrazine-3,8(2H,7H)-dione (**52**)*. Yield 77%; m.p. 286–288 °C (2-Methoxyethanol). ^{1}H NMR (DMSO-d_6) 5.27 (br s, 2H, NH_2), 6.64 (dd, 1H, ar, J = 1.5 Hz, J = 6.5 Hz), 6.82 (d, 1H, ar, J = 7.7 Hz), 6.84 (s, 1H, ar), 7.00 (s, 1H, H-5), 7.11 (t, 1H, ar, J = 7.8 Hz), 7.36 (t, 1H, ar, J = 7.4 Hz), 7.56 (t, 2H, ar, J = 7.6 Hz), 8.01 (d, 2H, ar, J = 7.7 Hz), 11.49 (br s, 1H, NH).

*4.1.4.2. 6-(4-Aminophenyl)-2-phenyl-1,2,4-triazolo[4,3-a]pyrazine-3,8(2H,7H)-dione (**53**)*. Yield 87%; m.p. > 300 °C (DMF/Acetone). ^{1}H NMR (DMSO-d_6) 5.49 (br s, 2H, NH_2), 6.61 (d, 2H, ar, J = 8.6 Hz), 7.00 (s, 1H, H-5), 7.37–7.33 (m, 3H, ar), 7.55 (t, 2H, ar, J = 7.6 Hz), 8.01 (d, 2H, ar, J = 7.7 Hz), 11.38 (br s, 1H, NH).

*4.1.5. General procedure for the synthesis of 8-chloro-2-phenyl-1,2,4-triazolo[4,3-a]pyrazin-3-(2H)-one derivatives **54–65**.*

A suspension of the suitable triazolopyrazin-3,8-dione derivatives **39–50** (2.1 mmol) in phosphorus oxychloride (12 mL) was heated under microwave irradiation at 170 °C for 1.5 h. The excess of phosphorus oxychloride was distilled off and the residue was treated with water (about 5–10 mL). The obtained solid was collected by filtration. These intermediates were pure enough (NMR, TLC) to be used for the next step without further purification.

*4.1.5.1. 8-Chloro-6-(2-furyl)-2-phenyl[1,2,4]triazolo[4,3-a]pyrazin-3-(2H)-one (**54**)*. Yield 90%; ^{1}H NMR (DMSO-d_6) 6.65–6.66 (d, 1H, furan proton), 6.98 (d, 1H, furan proton, J = 1.8 Hz), 7.39 (t, 1H, ar, J = 7.3 Hz), 7.58 (t, 2H, ar, J = 7.3 Hz), 7.83 (s, 1H, furan proton), 8.03 (d, 2H, ar, J = 7.1 Hz), 8.07 (s, 1H, H-5).

*4.1.5.2. 8-Chloro-6-(5-methylfuran-2-yl)-2-phenyl[1,2,4]triazolo[4,3-a] pyrazin-3-(2H)-one (**55**)*. Yield 92%; ^{1}H NMR (DMSO-d_6) 2.38 (s, 3H, CH_3), 6.28 (s, 1H, furan proton), 6.86 (s, 1H, furan proton), 7.41 (t, 1H, ar, J = 7.4 Hz), 7.59 (t, 2H, ar, J = 7.4 Hz), 7.96 (s, 1H, H-5), 8.05 (d, 2H, ar, J = 8.3 Hz).

*4.1.5.3. 8-Chloro-6-(2-thienyl)-2-phenyl[1,2,4]triazolo[4,3-a]pyrazin-3-(2H)-one (**56**)*. Yield 72%; ^{1}H NMR (DMSO-d_6) 7.18 (t, 1H, ar, J = 4.3 Hz), 7.41 (t, 1H, ar, J = 7.4 Hz), 7.58–7.65 (m, 3H, ar), 7.89 (d, 1H, thiophene proton, J = 3.6 Hz), 8.07 (d, 2H, ar, J = 8.3 Hz), 8.62 (s, 1H, H_{-5}).

*4.1.5.4. 8-Chloro-2-phenyl-6-(2-pyridyl)[1,2,4]triazolo[4,3-a]pyrazin-3-(2H)-one (**57**)*. Yield 87%; ^{1}H NMR (DMSO-d_6) 7.42 (t, 1H, ar, J = 7.1 Hz), 7.50 (t, 1H, ar, J = 6.1 Hz), 7.60 (t, 2H, ar, J = 7.8 Hz), 8.01–8.14 (m, 4H, ar), 8.62 (d, 1H, pyridine proton, J = 4.5 Hz), 8.71 (s, 1H, H_5).

*4.1.5.5. 8-Chloro-6-(2-methoxyphenyl)-2-phenyl-1,2,4-triazolo[4,3-a] pyrazin-3-(2H)-one (**58**)*. Yield 81%; ^{1}H NMR (DMSO-d_6) 3.98 (s, 3H, OCH_3), 7.13 (t, 1H, ar, 7.5 Hz), 7.21 (d, 1H, ar, J = 8.3 Hz), 7.38–7.45 (m, 2H, ar), 7.59 (t, 2H, ar, J = 7.8 Hz), 8.00 (d, 1H; ar, J = 7.8 Hz), 8.06 (d, 2H, ar, J = 8.2 Hz), 8.46 (s, 1H, H-5).

*4.1.5.6. 8-Chloro-6-(2-nitrophenyl)-2-phenyl-1,2,4-triazolo[4,3-a] pyrazin-3 (2H)-one (**59**)*. Yield 93%; ^{1}H NMR (DMSO-d_6) 7.45 (t, 1H, ar, J = 7.4 Hz), 7.63 (t, 2H, ar, J = 7.5 Hz), 7.76–7.75 (m, 1H, ar), 7.86–7.89 (m, 2H, ar), 8.06–8.08 (m, 3H, ar), 8.63 (s, 1H, H-5).

*4.1.5.7. 8-Chloro-6-(3-nitrophenyl)-2-phenyl-1,2,4-triazolo[4,3-a] pyrazin-3 (2H)-one (**60**)*. Yield 95%; ^{1}H NMR (DMSO-d_6) 7.42 (t, 1H, ar, J = 7.1 Hz), 7.60 (t, 2H, ar, J = 7.6 Hz), 7.79 (t, 1H, ar, J = 7.8 Hz), 8.07 (d, 2H, ar, J = 7.8 Hz), 8.26 (d, 1H, ar, J = 7.7 Hz), 8.54 (d, 1H, ar, J = 7.8 Hz), 8.82 (s, 1H, ar), 8.98 (s, 1H, H-5).

*4.1.5.8. 8-Chloro-6-(4-nitrophenyl)-2-phenyl-1,2,4-triazolo[4,3-a] pyrazin-3 (2H)-one (**61**)*. Yield 89%; ^{1}H NMR (DMSO-d_6) 7.42 (t, 1H, ar, J = 7.4 Hz), 7.61 (t, 2H, ar, J = 7.7 Hz), 8.07 (d, 2H, ar, J = 7.7 Hz), 8.32 (d, 2H, ar, J = 9.2 Hz), 8.36 (d, 2H, ar, J = 9.2 Hz), 8.95 (s, 1H, H-5).

*4.1.5.9. 6-(3-Bromophenyl)-8-chloro-2-phenyl-1,2,4-triazolo[4,3-a] pyrazin-3-(2H)-one (**62**)*. Yield 82%; ^{1}H NMR (DMSO-d_6) 7.36–7.41 (m, 2H, ar), 7.53–7.59 (m, 3H, ar), 7.82 (d, 1H, ar, J = 7.9 Hz), 7.09–7.11 (m, 2H, 1 ar + H-5), 8. 15 (d, 2H, ar, J = 7.7 Hz).

*4.1.5.10. 6-(4-Bromophenyl)-8-chloro-2-phenyl-1,2,4-triazolo[4,3-a] pyrazin-3-(2H)-one (**63**)*. Yield 93%; ^{1}H NMR (DMSO-d_6) 7.41 (t, 1H, ar, J = 7.3 Hz), 7.60 (t, 2H, ar, J = 8.1 Hz), 7.68 (d, 2H, ar, J = 8.5 Hz), 8.02 (d, 2H, ar, J = 8.5 Hz), 8.07 (d, 2H, ar, J = 8.6 Hz), 8.71 (s, 1H, H-5).

*4.1.5.11. 8-Chloro-6-(3-chlorophenyl)-2-phenyl-1,2,4-triazolo[4,3-a] pyrazin-3-(2H)-one (**64**)*. Yield 77%; ^{1}H NMR (DMSO-d_6) 7.41 (t, 1H, ar, J = 7.3 Hz), 7.47–7.54 (m, 2H, ar), 7.60 (t, 2H, ar, J = 7.4 Hz), 8.03–8.08 (m, 3H, ar), 8.13 (s, 1H, ar) 8.80 (s, 1H, H-5).

*4.1.5.12. 8-Chloro-6-(4-chlorophenyl)-2-phenyl-1,2,4-triazolo[4,3-a] pyrazin-3-(2H)-one (**65**)*. Yield 75%; ^{1}H NMR (DMSO-d_6) 7.40 (t, 1H, ar, J = 7.3 Hz), 7.53–7.61 (m, 4H, ar), 8.05–8.09 (m, 4H, ar), 8.69 (s, 1H, H-5).

*4.1.6. General procedure for the synthesis of 8-amino-6-aryl-2-phenyl-1,2,4-triazolo[4,3-a]pyrazin-3(2H)-one derivatives **1–12.***

A suspension of the 8-chloro-triazolopyrazine derivatives **54–65** (1.1 mmol) in a saturated ethanolic solution of NH_3 (50 mL) was heated at 140 °C in a sealed tube for 16 h, with the exception of the 6-(2-furyl) derivative **54** that was reacted at 100 °C for 4 h. The mixture was cooled at room temperature and the solid was collected by filtration, washed with water (about 5–10 mL), dried and recrystallized. Derivative **2** was purified by column chromatography (Cyclohexane/EtOAc, 6:4).

*4.1.6.1. 8-Amino-6-(2-furyl)-2-phenyl-1,2,4-triazolo[4,3-a]pyrazin-3-(2H)-one (**1**)*. Yield 25%; ^{1}H NMR (DMSO-d_6) 6.59–6.60 (m, 1H, furan ptoton), 6.78 (d, 1H, furan proton, J = 1.8 Hz), 7.38 (t, 1H, ar, J = 7.4 Hz), 7.41 (s, 1H, H-5), 7.58 (t, 2H, ar, J = 7.8 Hz), 7.65 (br s, 2H, NH_2), 7.74 (s, 1H, furan proton), 8.06 (d, 2H, ar, J = 7.8 Hz).

*4.1.6.2. 8-Amino-6-(5-methylfuran-2-yl)-2-phenyl-1,2,4-triazolo[4,3-a] pyrazin-3-(2H)-one (**2**)*. Yield 52%; m.p. 263–265 °C. ^{1}H NMR (DMSO-d_6) 2.34 (s, 3H, CH_3), 6.20 (s, 1H, furan proton), 6.66 (s, 1H, furan proton), 7.33–7.37 (m, 2H, 1ar + 1 furan proton), 7.56 (t, 2H, ar, J = 7.8 Hz), 7.63 (br s, 2H, NH_2), 8.06 (d, 2H, ar, J = 7.8 Hz). ^{13}C NMR (DMSO-d_6) 13.89, 99.15, 108.39, 108.79, 119.81, 126.78, 129.58, 129.65, 131.47, 137.88, 147.51, 148.27, 150.06, 152.30.

*4.1.6.3. 8-Amino-2-phenyl-6-(2-thienyl)-1,2,4-triazolo[4,3-a]pyrazin-3(2H)-one (**3**)*. Yield 58%; m.p. 283–284 °C (EtOH/2-Methoxyethanol). ^{1}H NMR (DMSO-d_6) 7.11 (t, 1H, ar, J = 4.4 Hz), 7.36 (t, 1H, ar, J = 7.5 Hz), 7.51–7.71 (m, 6H, 4ar + NH_2), 7.80 (s, 1H, H_5), 8.07 (d, 2H, ar, J = 7.8 Hz). IR 3318, 3223, 1715, 1643. ^{13}C NMR (DMSO-d_6) 100.20, 119.85, 123.09, 126.50, 126.79, 128.62, 129.67, 131.52, 132.25, 137.92, 142.42, 147.53, 147.92.

*4.1.6.4. 8-Amino-2-phenyl-6-(2-pyridyl)- 1,2,4-triazolo[4,3-a]pyrazin-3(2H)-one (**4**)*. Yield 62%; m.p. 251–252 °C (EtOH). ^{1}H NMR (DMSO-d_6) 7.36 (t, 2H, ar, J = 5.9 Hz), 7.57 (t, 2H, ar, J = 8.0 Hz), 7.65 (br s, 2H, NH_2), 7.90 (t, 1H, pyridine proton J = 3.9 Hz), 7.92–8.10 (m, 4H, 3ar + H_5), 8.62 (d, 1H, ar, J = 3.8 Hz). IR 3217, 3167, 1715, 1634.

*4.1.6.5. 8-Amino-6-(2-methoxyphenyl)-2-phenyl-1,2,4-triazolo[4,3-a] pyrazin-3(2H)-one (**5**)*. Yield 68%; m.p. 249–251 °C (EtOH). ^{1}H NMR (DMSO-d_6) 3.93 (s, 3H, OCH_3), 7.06 (t, 1H, ar, J = 8.1 Hz), 7.14 (d, 1H, ar, J = 8.1 Hz), 7.34–7.37 (m, 2H, ar), 7.48 (br s, 2H, NH_2), 7.56 (t, 2H, ar, J = 7.8 Hz), 7.9 (s, 1H, H-5), 8.06–8.09 (m, 3H, ar).

*4.1.6.6. 8-Amino-6-(2-nitrophenyl)-2-phenyl-1,2,4-triazolo[4,3-a] pyrazin-3 (2H)-one (**6**)*. Yield 83%; m.p. 281–283 °C (AcOH). ^{1}H NMR (DMSO-d_6) 7.40 (t, 1H, ar, J = 7. 4 Hz), 7.58–7.69 (m, 6H, 4ar + NH_2), 7.76–7.80 (m, 2H, 1 ar + H-5), 7.98 (d, 1H, ar, J = 7. 8 Hz), 8.09 (d, 2H, ar, J = 7.7 Hz).

*4.1.6.7. 8-Amino-6-(3-nitrophenyl)-2-phenyl-1,2,4-triazolo[4,3-a] pyrazin-3 (2H)-one (**7**)*. Yield 72%; m.p. 280–281 °C (AcOH). ^{1}H NMR (DMSO-d_6) 7.37 (t, 1H, ar, J = 7.2 Hz), 7.57 (t, 2H, ar, J = 7.6 Hz), 7.71 (t, 1H, ar, J = 7.7 Hz), 7.77 (br s, 2H, NH_2), 8.07–8.09 (m, 3H, 2

ar + H-5), 8.19 (d, 1H, ar, J = 7.6 Hz), 8.48 (d, 1H, ar, J = 7.6 Hz), 8.85 (s, 1H, ar).

4.1.6.8. 8-Amino-6-(4-nitrophenyl)-2-phenyl-1,2,4-triazolo[4,3-a] pyrazin-3 (2H)-one ***(8)***. Yield 69%; m.p. 297–299 °C (2-Methoxyethanol/DMF). ^{1}H NMR (DMSO-d_6) 7.36 (t, 1H, ar, J = 7.4 Hz), 7.57 (t, 2H, ar, J = 7.7 Hz), 7.73 (br s, 2H, NH_2), 8.06–8.08 (m, 3H, 2 ar + H-5), 8.28 (s, 4H, ar). ^{13}C NMR (DMSO-d_6) 104.87, 119.91, 124.19, 126.80, 126.87, 129.69, 131.56, 133.78, 137.85, 143.48, 147.17, 147.64, 148.08. IR 1713, 3373, 3485.

4.1.6.9. 8-Amino-6-(3-bromophenyl)-2-phenyl-1,2,4-triazolo[4,3-a] pyrazin-3(2H)-one ***(9)***. Yield 87%; m.p. 281–283 °C (2-Methoxyethanol). ^{1}H NMR (DMSO-d_6) 7.35–7.40 (m, 2H, ar), 7.52–7.59 (m, 3H, ar), 7.66 (br s, 2H, NH_2), 7.93 (s, 1H, H-5), 8.02 (d, 1H, ar, J = 7.8 Hz), 8.07 (d, 2H, ar, J = 8.0 Hz), 8.23 (s, 1H, ar). ^{13}C NMR (DMSO-d_6) 102.93, 119.90, 122.57, 124.64, 126.83, 128.65, 129.68, 131.04, 131.09, 131.60, 134.18, 137.89, 139.26, 147.63, 147.94.

4.1.6.10. 8-Amino-6-(4-bromophenyl)-2-phenyl-1,2,4-triazolo[4,3-a] pyrazin-3(2H)-one ***(10)***. Yield 92%; m.p. 266–268 °C (2-Methoxyethanol). ^{1}H NMR (DMSO-d_6) 7.36 (t, 1H, ar, J = 7.4 Hz), 7.57 (t, 2H, ar, J = 7.8 Hz), 7.63–7.61 (m, 4H, 2 ar + NH_2), 7.85 (s, 1H, H-5), 7.96 (d, 2H, ar, J = 8.6 Hz), 8.07 (d, 2H, ar, J = 7.8 Hz). ^{13}C NMR (DMSO-d_6) 102.35, 119.89, 121.63, 126.79, 128.01, 129.66, 131.57, 131.81, 134.82, 136.15, 137.93, 147.63, 147.94.

4.1.6.11. 8-Amino-6-(3-chlorophenyl)-2-phenyl-1,2,4-triazolo[4,3-a] pyrazin-3(2H)-one ***(11)***. Yield 85%; m.p. 279–281 °C (EtOH/2-Methoxyethanol). ^{1}H NMR (DMSO-d_6) 7.34–7.47 (m, 3H, ar), 7.57 (t, 2H, ar, J = 7.7 Hz), 7.65 (br s, 2H, NH_2), 7.92 (s, 1H, H-5), 7.98 (d, 1H, ar, J = 7. 7 Hz), 8.06–8.08 (m, 3H, ar). ^{13}C NMR (DMSO-d_6) 102.96, 119.92, 124.30, 125.78, 126.82, 128.14, 129.67, 130.78, 131.62, 133.96, 134.33, 137.91, 139.09, 147.64, 147.95.

4.1.6.12. 8-Amino-6-(4-chlorophenyl)-2-phenyl-1,2,4-triazolo[4,3-a] pyrazin-3(2H)-one ***(12)***. Yield 87%; m.p. 256–258 °C (2-Methoxyethanol). ^{1}H NMR (DMSO-d_6) 7.36 (t, 1H, ar, J = 7.4 Hz), 7.48 (d, 2H, ar, J = 8.6 Hz), 7.56 (t, 2H, ar, J = 7.6 Hz), 7.63 (br s, 2H, NH_2), 7.84 (s, 1H, H-5), 8.02 (d, 2H, ar, J = 8.5 Hz), 8.07 (d, 2H, ar, J = 7.6 Hz). ^{13}C NMR (DMSO-d_6) 102.40, 119.88, 127.70, 128.97, 129.57, 129.72, 131.55, 132.99, 134.75, 135.76, 137.92, 147.62, 147.92.

4.1.7. 8-Amino-6-(2-hydroxyphenyl)-2-phenyl-1,2,4-triazolo[4,3-a] pyrazin-3(2H)-one ***13.***

1 M solution of BBr_3 in dichloromethane (5.1 mL) was slowly added at 0 °C, under nitrogen atmosphere, to a suspension of the methoxy-substituted triazolopirazine **5** (1.0 mmol) in anhydrous dichloromethane (20 mL). The mixture was stirred at room temperature for about 30 h, then was diluted with water (10 mL) and neutralized with a $NaHCO_3$ saturated solution. The organic solvent was removed by evaporation at reduced pressure and the solid was collected by filtration. The crude derivative was dried and purified by recrystallization. Yield 88%; m.p. 274–276 °C (EtOH). ^{1}H NMR (DMSO-d_6) 6.83–6.87 (m, 2H, ar), 7.18 (t, 1H, ar, J = 8.1 Hz), 7.37 (t, 1H, ar, J = 7.8 Hz), 7.57 (t, 2H, ar, J = 8.0 Hz), 7.91–7.93 (m, 4H, 1ar + H-5 + NH_2), 8.07 (d, 2H, ar, J = 8. 0 Hz). 11.93 (s, 1H, OH). ^{13}C NMR (DMSO-d_6) 102.57, 117.76, 119.46, 119.61, 119.90, 126.87, 127.18, 129.70, 129.87, 131.27, 134.75, 137.88, 147.12, 147.59, 157.06.

4.1.8. General procedure for the synthesis of 8-amino-6-(aminophenyl)-2-phenyl-1,2,4-triazolo[4,3-a]pyrazin-3-(2H)ones ***14–16***.

10% Pd/C (10% w/w with respect to the nitro derivative) was added to a solution of the 6-(nitrophenyl) derivatives **6–8** (1.2 mmol) in DMF (10 mL). The mixture was hydrogenated in a Parr apparatus at 40 psi for 24 h. Then the catalyst was filtered off and the clear solution was diluted with water (about 50 mL) to obtain a solid that was collected by filtration, washed with water and Et_2O, dried and recrystallized.

4.1.8.1. 8-Amino-6-(2-aminophenyl)-2-phenyl-1,2,4-triazolo[4,3-a] pyrazin-3 (2H)-one ***(14)***. Yield 59%; m.p. 256–258 °C (2-Methoxyethanol). ^{1}H NMR (DMSO-d_6) 5.78 (br s, 2H, NH_2), 6.58 (t, 1H, ar, J = 7.4 Hz), 6.72 (d, 1H, ar, J = 8. 0 Hz), 7.05 (t, 1H, ar, J = 7.2 Hz), 7.30–7.38 (m, 3H, 2 ar + H-5), 7.56 (t, 2H, ar, J = 7.9 Hz), 7.62 (br s, 2H, NH_2), 8.07 (d, 2H, ar, J = 7.9 Hz).

4.1.8.2. 8-Amino-6-(3-aminophenyl)-2-phenyl-1,2,4-triazolo[4,3-a] pyrazin-3 (2H)-one ***(15)***. Yield 75%; m.p. 280–282 °C (2-Methoxyethanol). ^{1}H NMR (DMSO-d_6) 5.10 (br s, 2H, NH_2), 6.54–6.57 (m, 1H, ar), 7.04–7.10 (m, 2H, ar), 7.16 (s, 1H, ar), 7.36 (t, 1H, ar, J = 7.4 Hz), 7.50 (s, 1H, H-5), 7.51 (br s, 2H, NH_2), 7.56 (t, 2H, ar, J = 7.7 Hz), 8.08 (d, 2H, ar, J = 7.7 Hz).

4.1.8.3. 8-Amino-6-(4-aminophenyl)-2-phenyl-1,2,4-triazolo[4,3-a] pyrazin-3 (2H)-one ***(16)***. Yield 78%; m.p. 294–296 °C (CH_3NO_2/DMF). ^{1}H NMR (DMSO-d_6) 5.27 (br s, 2H, NH_2), 6.59 (d, 2H, ar, J = 8.6 Hz), 7.35 (t, 1H, ar, J = 7.4 Hz), 7.44 (br s, 2H, NH_2), 7.46 (s, 1H, H-5), 7.56 (t, 2H, ar, J = 8. 5 Hz), 7.64 (d, 2H, ar, J = 8.6 Hz), 8.08 (d, 2H, ar, J = 7. 6 Hz). ^{13}C NMR (DMSO-d_6) 149.40, 147.56, 147.54, 138.03, 136.93, 131.50, 129.64, 126.89, 126.68, 124.15, 119.83, 114.10, 98.70. IR 1703, 3292–3115, 3350, 3435.

4.1.9. General procedure for the synthesis of 8-amino-2-phenyl-6-(piperazinylphenyl)-1,2,4-triazolo[4,3-a]pyrazin-3-(2H)one ***17–19***

A suspension of the 8-amino-6-(aminophenyl) derivatives **14–16** (1.1 mmol) and bis-(2-chloroethyl)amine hydrochloride in sulfolane (5 mL) was heated at 150 °C until the disappearance of starting material (TLC- monitoring 16–24 h). After cooling at 0–5 °C, the mixture was treated with acetone (30 mL) and the obtained ammonium salts were collected by filtration and dissolved in water (50 mL). The solution was neutralized with a $NaHCO_3$ saturated solution and extracted with EtOAc (40 mL × 5). The organic phase was anhydrified (Na_2SO_4) and reduced to dryness under vacuum to give a yellow solid. All the crude derivatives were purified by recrystallization.

4.1.9.1. 8-Amino-2-phenyl-6-(2-piperazin-1-yl-phenyl)-1,2,4-triazolo[4,3-a]pyrazin-3-(2H)one ***(17)***. Yield 52%; m.p. 214–216 °C (CH_3NO_2). ^{1}H NMR (DMSO-d_6) 2.82 (s, 8H, 4 CH_2), 7.08–7.11 (m, 2H, ar), 7.28 (t, 1H, ar, J = 7.6 Hz), 7.36 (t, 1H, ar, J = 7.4 Hz), 7.51 (br s, 2H, NH_2), 7.56 (t, 2H, ar, J = 7.7 Hz), 7.84 (d, 1H, ar, J = 6.6 Hz), 8.09 (d, 2H, ar, J = 7.8 Hz), 8.40 (s, 1H, H-5).

4.1.9.2. 8-Amino-2-phenyl-6-(3-piperazin-1-yl-phenyl)-1,2,4-triazolo[4,3-a]pyrazin-3-(2H)one ***(18)***. Yield 47%; m.p. 234–235 °C (CH_3NO_2). ^{1}H NMR (DMSO-d_6) 2.86 (t, 4H, 2 CH_2, J = 4. 9 Hz), 3.11 (t, 4H, 2 CH_2, J = 5.1 Hz), 6. 90 (dd, 1H, ar, J = 6.3 Hz, J = 1.9 Hz), 7.25 (t, 1H, ar), 7.34–7.39 (m, 2H, ar), 7.51–7.58 (m, 5H, 3 ar + NH_2), 7.77 (s, 1H, H-5), 8.08 (d, 2H, ar, J = 8.6 Hz).

4.1.9.3. 8-Amino-2-phenyl-6-(4-(piperazin-1-yl-)phenyl)-1,2,4-triazolo [4,3-a]pyrazin-3-(2H)one ***(19)***. Yield 56%; m.p. 255–257 °C (CH_3NO_2). ^{1}H NMR (DMSO-d_6) ^{1}H NMR (DMSO-d_6) 2.84 (t, 4H, 2 CH_2, J = 4.9 Hz), 3.11 (t, 4H, 2 CH_2, J = 5.1 Hz), 7. 96 (d, 2H, ar, J = 8.9 Hz), 7.36 (t, 1H, ar, J = 7.4 Hz), 7. 50 (br s, 2H, NH_2), 7.54–7.59 (m, 2H, 1 ar + H-5), 7.82 (d, 2H, ar, J = 8.8 Hz), 8.08 (d, 2H, ar, J = 7.7 Hz).

4.1.10. 4-(3-(8-Amino-3-oxo-2-phenyl-2,3-dihydro-1,2,4-triazolo[4,3-a] pyrazin-6-yl)phenyl)-1,1-dimethyl-piperazin-1-ium ***20***.

A mixture of compound **18** (0.4 mmol), methyl iodide (0.7 mmol) and potassium carbonate in anhydrous DMF (0.5 mL) was stirred at

room temperature for 7 h, then it was diluted with H_2O (about 50 mL) and EtOAc (about 40 mL). The obtained solid was collected by filtration and recristallized. Yield 35%; m.p. > 300 °C (DMF). ^{1}H NMR (DMSO-d_6) 3.23 (s, 6H, 2CH_3), 3.61 (br s, 8H, piperazine protons), 7.02 (d, 1H, ar, J = 7.6 Hz), 7.32–7.38 (m, 2H, ar), 7.52–7.59 (m, 6H, 4 ar + NH_2), 7.87 (s, 1H, H-5), 8.07 (d, 2H, ar, J = 8.2 Hz).

*4.1.11. General procedure for the synthesis of 8-amino-6-(benzylpiperazin-1-yl-phenyl)-2-phenyl-1,2,4-triazolo[4,3-a]pyrazin-3-(2H)one **21** and **22**.*

A suspension of the 8-amino-6-(piperazinyl)phenyl derivative **18** or **19** (0.7 mmol), anhydrous triethylamine (0.9 mmol) and benzylchloride (0.9 mmol) in anhydrous dioxane (10 mL) was heated at reflux until the disappearance of starting material (TLC monitoring, 24–48 h). In case of compound **21**, the organic solvent was removed by evaporation at reduced pressure and the residue treated with EtOAc (50 mL). The organic phase was washed with water (30 mL × 3), anhydrified (Na_2SO_4) and reduced to dryness under vacuum to give a solid. To isolate compound **22**, the solvent was evaporated under vacuum and the residue was treated with water (30 mL). The resulting solid was collected by filtration and washed with diethyl ether (about 20 mL). The crude product was purified by recrystallization (**21**) or column chromatography (**22**, eluent Cyclohexane/EtOAc/MeOH, 5.5:4.5:0.1).

*4.1.11.1. 8-Amino-6-[3-(benzylpiperazin-1-yl)phenyl]-2-phenyl-1,2,4-triazolo[4,3-a]pyrazin-3-(2H)one **(21)**.* Yield 34%; m.p. 208–210 °C (EtOH). ^{1}H NMR (DMSO-d_6) 2.55 (t, 4H, 2 CH_2, J = 4. 8 Hz), 3.22 (t, 4H, 2 CH_2, J = 4.9 Hz), 6.91 (dd, 1H, ar, J = 6.2, J = 2.0 Hz), 7.24–7.30 (m, 2H, ar), 7.34–7.31 (m, 6H, ar), 7.52–7.59 (m, 5H, 3 ar + NH_2), 7.77 (s, 1H, H-5), 8.08 (d, 2H, ar, J = 7.6 Hz).

*4.1.11.2. 8-Amino-6-[4-(benzylpiperazin-1-yl)phenyl]-2-phenyl-1,2,4-triazolo[4,3-a]pyrazin-3-(2H)one **(22)**.* Yield 63%; m.p. 244–246 °C (EtOH). ^{1}H NMR ($CDCl_3$) 2.65 (t, 4H, 2 CH_2, J = 4. 8 Hz), 3.30 (t, 4H, 2 CH_2, J = 4.9 Hz), 5.54 (br s, 2H, NH_2), 6.98 (d, 2H, ar, J = 8.8 Hz), 7.30–7.40 (m, 6H, ar), 7.52 (t, 2H, ar, J = 7.7 Hz), 7.60 (s, 1H, H-5), 7.76 (d, 2H, ar, J = 8.8 Hz), 8.12 (d, 2H, ar, J = 7.8 Hz). ^{13}C NMR (DMSO-d_6) 48.63, 52.95, 63.07, 101.56, 11.64, 119.84, 126.64, 126.85, 127.21, 128.32, 129.19, 129.24, 130.81, 136.62, 137.58, 146.38, 147.47, 151.50.

*4.1.12. Ethyl 2-amino-2-benzylhydrazonoacetate **66***

Ethyl thiooxamate (3.7 mmol) was added to a mixture of benzylhydrazine hydrochloride (3.7 mmol) and K_2CO_3 (3.7 mmol) in absolute ethanol (15 mL). The suspension was stirred at 25 °C for 15 h, then was treated with $NaHCO_3$ saturated solution (40 mL) and extracted with EtOAc (30 mL × 3). The organic layer was washed with brine (30 mL × 3), anhydrified (Na_2SO_4) and evaporated under reduced pressure to give a brown solid which was used for the next step without further purification. Yield 88%; ^{1}H NMR (DMSO-d_6) 1.22 (t, 3H, CH_3, J = 7.1 Hz), 4.16 (q, 2H, CH_2, J = 7. 1 Hz), 4.25 (d, 2H, CH_2, J = 5.1 Hz), 5.49 (br s, 2H, NH_2), 5.88 (t, 1H, NH, J = 5.1 Hz), 7.24–7.35 (m, 5H, ar).

*4.1.13. Synthesis of ethyl 5-oxo-1-benzyl-4,5-dihydro-1H-1,2,4-triazole-3-carboxylate **67**.*

Carbonyldiimidazole (5.4 mmol) was portion wise added to a cold (T = 0° C) suspension of ethyl 2-amino-2-benzylhydrazonoacetate **66** (2.7 mmol) in anhydrous CH_2Cl_2 (20 mL). The mixture was stirred at room temperature for 15 h, then was treated with a NH_4Cl saturated solution (30 mL) and extracted with CH_2Cl_2 (30 mL × 3). The organic phase was anhydrified (Na_2SO_4) and the solvent was evaporated under reduced pressure to afford a yellow solid which was purified by column chromatography (cyclohexane/EtOAc/MeOH, 6:4:1). Yield 35%; mp 154–156 °C. ^{1}H NMR (DMSO-d_6) 1.27 (t, 3H, CH_3, J = 7.1 Hz), 4.31 (q, 2H, CH_2, J = 7.1 Hz), 4.95 (s, 2H, CH_2), 7.26–7.38 (m, 5H, ar), 12.67 (br s, 1H, NH).

*4.1.14. General procedure for the synthesis of 1-benzyl-4-(2-phenyl/heteroaryl-2-oxoethyl)-5-oxo-4,5-dihydro-1H-1,2,4-triazole-3-carboxylate derivatives **68–70***

The title compounds were synthesized by reacting ethyl 1-benzyl-5-oxo-1,2,4-triazole-3-carboxylate **67** (1 mmol) with phenacyl bromide or heteroaryl-α-bromoketone [38–39] (1.2 mmol) in the same conditions described above to prepare compounds **27–38** from **26**. The crude **68**, **69** and **70** were purified by column chromatography (eluent *n*-Hexane/Et_2O/MeOH/Toluene 2:5.5:0.1:0.5, Cyclohexane/EtOAc 6:4 and Cyclohexane/EtOAc 1:1, respectively).

*4.1.14.1. Ethyl 1-benzyl-5-oxo-4-[2-oxo-2-phenylethyl]-1-phenyl-4,5-dihydro-1H-1,2,4-triazole-3-carboxylate **(68)**.* Yield 34%; m.p. 90–92 °C. ^{1}H NMR ($CDCl_3$) 1.34 (t, 3H, CH_3, J = 7.1 Hz), 4.36 (q, 2H, CH_2, J = 7.1 Hz), 5.15 (s, 2H. CH_2), 5.51 (s, 2H. CH_2), 7.32–7.42 (m, 5H, ar), 7.54 (t, 2H, ar, J = 7.7 Hz), 7.67 (t, 1H, ar, J = 7.5 Hz), 8.01 (d, 2H, J = 7.7 Hz).

*4.1.14.2. Ethyl 1-benzyl-4-[2-(furan-2-yl)-2-oxoethyl]-5-oxo-4,5-dihydro-1H-1,2,4-triazole-3-carboxylate **(69)**.* Yield 68%; m.p. 104–106 °C. ^{1}H NMR ($CDCl_3$) 1.34 (t, 3H, CH_3, J = 7.1 Hz), 4.36 (q, 2H, CH_2, J = 7.1 Hz), 5.13 (s, 2H. CH_2), 5.37 (s, 2H. CH_2), 6.63 (dd, 1H, furan proton, J = 1.6 Hz, J = 1.9 Hz), 7.32–7.41 (m, 6H, 5ar + 1 furan proton), 7.67 (s, 1H, furan proton).

*4.1.14.3. Ethyl 1-benzyl-4-[2-(5-methylfuran-2-yl)-2-oxoethyl]-5-oxo-4,5-dihydro-1H-1,2,4-triazole-3-carboxylate **(70)**.* Yield 93%; Oily compound. ^{1}H NMR ($CDCl_3$) 1.35 (t, 3H, CH_3, J = 7.1 Hz), 2.44 (s, 3H, CH_3), 4.37 (q, 2H, CH_2, J = 7.1 Hz), 5.13 (s, 2H, CH_2), 5.33 (s, 2H, CH_2), 6.24 (d, 1H, furan proton, J = 3.3 Hz), 7.25 (d, 1H, 1 furan proton, J = 3.4 Hz), 7.41–7.31 (m, 5H, ar).

*4.1.15. General procedure for the synthesis of 2-benzyl-1,2,4-triazolo[4,3-a]pyrazine-3,8(2H,7H)-dione derivatives **71–73**.*

The title compounds were synthesized from ethyl 1,2,4-triazole-3-carboxylate derivatives **68–70** (0.9 mmol) and anhydrous ammonium acetate (3.5 mmol), in the same conditions described above to prepare compounds **39–50** from **27 to 38**.

*4.1.15.1. 2-Benzyl-6-phenyl-1,2,4-triazolo[4,3-a]pyrazine-3,8(2H,7H)-dione **(71)**.* Yield 32%; m.p. 278–279 °C (2-Methoxyethanol). ^{1}H NMR (DMSO-d_6) 5.13 (s, 2H, CH_2), 7.20 (s, 1H, H-5), 7.35–7.38 (m, 5H, ar), 7.45–7.47 (m, 3H, ar), 7.68–7.69 (m, 2H, ar), 11.49 (br s, 1H, NH).

*4.1.15.2. 2-Benzyl-6-(furan-2-yl)-1,2,4-triazolo[4,3-a]pyrazine-3,8(2H,7H)-dione **(72)**.* Yield 81%; m.p. 280–282 °C (AcOH). ^{1}H NMR (DMSO-d_6) 5.11 (s, 2H, CH_2), 6.63 (dd, 1H, furan proton, J = 1.6 Hz, J = 1.8 Hz), 7.11 (s, 1H, H-5), 7.16 (d, 1H, ar, J = 3.4 Hz), 7.32–7.39 (m, 5H, 4ar + 1 furan proton), 7.8 (s, 1H, furan proton), 11.56 (br s, 1H, NH).

*4.1.15.3. 2-Benzyl-6-(5-methylfuran-2-yl)-1,2,4-triazolo[4,3-a]pyrazine-3,8(2H,7H)-dione **(73)**.* Yield 28%; m.p. 286–288 °C (AcOH). ^{1}H NMR (DMSO-d_6) 2.32 (s, 3H, CH_3), 5.11 (s, 2H, CH_2), 6.22 (s, 1H, furan proton), 7.01 (s, 1H, furan proton), 7.03 (s, 1H, H-5), 7.34–7.37 (m, 5H, ar), 11.46 (br s, 1H, NH).

*4.1.16. General procedure for the synthesis of 2-benzyl-8-chloro-1,2,4-triazolo[4,3-a]pyrazin-3-(2H)-one derivatives **74–76**.*

The title compounds were synthesized by heating a suspension of the suitable triazolopyrazin-3,8-dione derivatives **71–73** (2.1 mmol) in phosphorus oxychloride (12 mL) in the same conditions described above to prepare compounds **54–65** from **39 to 50**. These intermediates were pure enough (NMR, TLC) to be used for the next step without further purification.

*4.1.16.1. 2-Benzyl-8-chloro-6-phenyl-1,2,4-triazolo[4,3-a]pyrazin-3-(2H)-one (**74**).* Yield 68%; ^{1}H NMR (DMSO-d_6) 5.24 (s, 2H, CH_2), 7.33–7.42 (m, 6H, ar), 7.48 (t, 2H, ar, J = 7.1), 8.01 (d, 2H, ar, *J* = 7.2 Hz), 8.53 (s, 1H, H-5).

*4.1.16.2. 2-Benzyl-8-chloro-6-(furan-2-yl)-1,2,4-triazolo[4,3-a]pyrazin-3-(2H)-one (**75**).* Yield 85%; ^{1}H NMR (DMSO-d_6) 5.22 (s, 2H, CH_2), 6.65 (dd, 1H, furan proton, *J* = 1.7 Hz, *J* = 1.5 Hz), 6.95 (d, 1H, furan proton, *J* = 3.2 Hz), 7.36–7.41 (m, 5H, ar), 7.82 (s, 1H, furan proton), 8.02 (s, 1H, H-5).

*4.1.16.3. 2-Benzyl-8-chloro-6-(5-methylfuran-2-yl)-1,2,4-triazolo[4,3-a] pyrazin-3-(2H)-one (**76**).* Yield 95%; ^{1}H NMR (DMSO-d_6) 2.36 (s, 3H, CH_3), 5.22 (s, 2H, CH_2), 6.25 (d, 1H, furan proton, *J* = 2.1 Hz), 6.81 (d, 1H, furan proton, *J* = 2.8 Hz), 7.33–7.38 (m, 5H, ar), 7.89 (s, 1H, H-5).

*4.1.17. General procedure for the synthesis of 8-amino-6-aryl-2-phenyl-1,2,4-triazolo[4,3-a]pyrazin-3(2H)-one derivatives **23–35**.*

The title compounds were obtained by heating the 8-chloro-triazolopyrazine derivatives **74–76** (1.1 mmol) in a saturated ethanolic solution of NH_3 (50 mL) in the same conditions described above to prepare derivatives **1–12**. The crude compounds **24** and **25** were purified by column chromatography (*n*-Hexane/EtOAc/MeOH, 7:3:0.1 and Cyclohexane/EtOAc/MeOH, 5:4:1).

*4.1.17.1. 8-Amino-2-benzyl-6-phenyl-1,2,4-triazolo[4,3-a]pyrazin-3(2H)-one (**23**).* Yield 79%; m.p. 288–290 °C (DMF). ^{1}H NMR (DMSO-d_6) 5.18 (s, 2H, CH_2), 7.31–7.45 (m, 10H, 8 ar + NH_2), 7.72 (s, 1H, H-5), 7.95 (d, 2H, ar, *J* = 7.2 Hz).

*4.1.17.2. 8-Amino-2-benzyl-6-(furan-2-yl)-1,2,4-triazolo[4,3-a]pyrazin-3(2H)-one (**24**).* Yield 38%; m.p. 185–187 °C. ^{1}H NMR (DMSO-d_6) 5.16 (s, 2H, CH_2), 6.58 (dd, 1H, furan proton, *J* = 1.6 Hz, *J* = 1.8 Hz), 6.75 (d, 1H, furan proton, *J* = 3.1 Hz), 7.31–7.37 (m, 6H, 5 ar + H-5), 7.51 (br s, 2H, NH_2), 7.72 (s, 1H, furan proton).

*4.1.17.3. 8-Amino-2-benzyl-6-(5-methylfuran-2-yl)-1,2,4-triazolo[4,3-a] pyrazin-3-(2H)-one (**25**).* Yield 54%; m.p. 215–217 °C. ^{1}H NMR (DMSO-d_6) 2.33 (s, 3H, CH_3), 5.15 (s, 2H, CH_2), 6.17–6.18 (m, 1H, furan proton), 6.61 (d, 1H, furan proton, *J* = 3.0 Hz),. 7.30–7.39 (m, 6H, ar + H-5), 7.47 (br s, 2H, NH_2).

4.2. Pharmacology

4.2.1. Binding assays

4.2.1.1. Cell culture. CHO cells stable transfected with hARs were grown in Dulbecco's modified Eagle's medium (DMEM) with nutrient mixture F12 supplemented with 10% fetal bovine serum (FBS), 100 U/ml penicillin, 100 μg/ml streptomycin, 2.5 μg/ml Amphotericin B, 0.1 mg/ml Geneticine and 1 mM Sodium Pyruvate. They were cultured at 37 °C in a humidified atmosphere of 5% CO_2/95% air [40].

4.2.1.2. Membrane preparation. Crude membranes for radioligand binding experiments were prepared by collecting cells (CHO stably transfected with hA_1, hA_{2A} and hA_3 ARs) in ice-cold hypotonic buffer (5 mM Tris/HCl, 2 mM EDTA, pH 7.4). The cell suspension was homogenized on ice (Ultra-Turrax, 2 × 20 sec at full speed) and the homogenate was spun for 10 min (4 °C) at 3200 rpm. The supernatant was centrifuged for 50 min at 37,000 rpm at 4 °C. The membrane pellet was resuspended in the specific binding buffer (hA_1ARs: 50 mM Tris/HCl buffer pH 7.4; hA_{2A}ARs: 50 mM Tris/HCl, 50 mM $MgCl_2$ pH 7.4; hA_3ARs: 50 mM Tris/HCl, 10 mM $MgCl_2$, 1 mM EDTA, pH 8.25), frozen in liquid nitrogen at a protein concentration of 2–4 mg/ml and stored at −80 °C.

4.2.1.3. Radioligand binding. Dissociation constants of radioligands (K_D values) were obtained from saturation binding experiments. Dissociation constants of unlabelled compounds (K_i values) were determined in radioligand competition experiments.

For saturation binding, increasing concentration of the radioligands [^{3}H]CCPA ([^{3}H]2-chloro-*N*^{6}–cyclopentyladenosine, hA_1 ARs), [^{3}H] NECA ([^{3}H]5′-N-ethylcarboxamidoadenosine, hA_{2A} ARs), and [^{3}H] HEMADO ([^{3}H]2-(1-Hexynyl)-N-methyladenosine, hA_3 ARs) were incubated, in a 96-well plate, in a total volume of 200 μl containing 0.2 U/ml adenosine deaminase and 10 μg of membrane proteins in the specific buffer of each receptor.

In competition experiments, a fixed concentration of radioligand (1 nM [^{3}H]CCPA, K_D = 1.1 nM; 10 nM [^{3}H]NECA, K_D = 20 nM; [^{3}H] HEMADO, K_D = 1.5 nM) was incubated in a 96-well plate with 10 μg of specific receptor cell membrane preparations and increasing concentrations of the compound understudy. Non-specific binding was determined in the presence of 1 mM theophylline for hA_1 AR and 100 μM (R)-N^6-phenyliso-propyladenosine (R-PIA) for both hA_{2A} AR and hA_3 AR. Samples were incubated for 3 h at rt, filtered using a microplate format utilizing the 96-well microplate filtration system Microbeta Filtermat 96 Cell Harvester (PerkinElmer) to separate the free fractions to the bound fractions. The filters were washed three times with 200 μl of ice-cold binding buffer specific for each receptor and subsequently dried. After the addition of 20 μl of scintillation cocktail, the bound radioactivity was determined using a Perkin Elmer Microbeta^2 scintillation counter. All binding data were calculated by non-linear curve fitting with Prism 5.0 programme (GraphPAD Software, San Diego, CA, USA). Each concentration was tested three-five times in triplicate and the values are given as the mean ± standard error (S.E.). Radioligand binding at the hA_{2B} AR is problematic because no high-affinity radioligand is commercially available for this subtype. Therefore, inhibition of NECA-stimulated adenylyl cyclase (cAMP assay, see below) was determined as a measurement of affinity of compounds.

4.2.2. GloSensor cAMP Assay

Cells, stably expressing the hA_1, hA_{2A}, and hA_{2B} ARs and transiently the biosensor, were harvested in CO_2-independent medium and were counted in a Neubauer chamber. The desired number of cells was incubated in equilibration medium containing a 3% v/v GloSensor cAMP reagent stock solution, 10% FBS, and 87% CO_2 independent medium. After 2 h of incubation at rt, the cells were dispensed in the wells of a 384-well plate and, when a steady-state basal signal was obtained, the NECA reference agonist or the understudy compounds, at different concentrations, were added. Initially, the ability of compounds **10**, **11** and **25** to stimulate (A_{2A} and A_{2B} ARs) or inhibit (A_1 AR) the cAMP production was evaluated, but any results were obtained. Subsequently, their antagonist profile was evaluated by assessing their ability to counteract NECA-induced increase (A_{2A} and A_{2B} ARs) or decrease (A_1 AR) of cAMP accumulation. The cells were incubated in the reaction medium (10 min at rt) with different understudy molecule concentrations and then treated with a fixed concentration of NECA. In the case of hA_1 AR, Forskolin (FSK) 10 μM was added 10 min after the agonist NECA and various luminescence reads were performed at different incubation times [40,41].

4.2.3. Statistical analysis

Responses were expressed as percentage of the maximal relative luminescence units (RLU). Concentration–response curves were fitted by a nonlinear regression with the Prism 5.0 programme (GraphPAD Software, San Diego, CA, USA). The antagonist profile of the two compounds was expressed as IC_{50}. The IC_{50} value is the concentration of antagonists that produces 50% inhibition of the agonist effect. Each concentration was tested three-five times in triplicate and the values are given as the mean ± S.E [42].

4.2.4. β-Amyloid-induced toxicity studies in SH-SY5Y cell lines

Human neuroblastoma SH-SY5Y cell line, was purchased by Istituto Zooprofilattico dell'Emilia e della Romagna (Brescia, Italy). Cells were

routinely cultured in DMEM High Glucose/Ham's F12 Mixture Medium (1:1) supplemented with 10% foetal bovine serum (FBS), 2 mM L-Glutamine (EuroClone S.p.a., Milano, Italy) at 37 °C, 5% CO_2 in humidified atmosphere. The growth medium was changed every 2–3 days. Cell damage (1×10^4 cell/well) was induced by incubation (24–72 h) with Aβ-amyloid peptide (Aβ fragment 25–35 aa (Sigma-Aldrich, Italy); 2 and 10 μM) after a previous aggregation period of 3 or 7 days at 37 °C. The studied compounds were co-incubated with Aβ-amyloid peptide (2 or 10 μM, previously aggregated for 7 days) for 48 h. Cell viability was evaluated by the reduction of 3-(4,5-di-methylthiozol-2-yl)-2,5-diphenyltetrazolium bromide (MTT) as an index of mitochondrial functional activity. Briefly, SH-SY5Y cells were seeded into 96 well plates at a density of 10,000 cells/well in complete growth medium for 1 day. After the above described treatments, the medium was removed and 1 mg/mL MTT was added into each well and incubated for at least 20 min at 37 °C. Following the removing of the chromogenic solution, the formazan crystals were dissolved in 50 μl of dimethyl sulfoxide (DMSO) and the absorbance was measured at 595 nm by a Multiscan FC photometer (ThermoFisher Scientific, Milano, Italy). Three independent experiments were conducted and each experiment was performed in quintuplicate. Viability was expressed as % in comparison to the control cells (arbitrarily set 100% of viable cells).

Statistical analyses were performed by One-way ANOVA followed by the Bonferroni test. All assessments were made by researchers blinded to treatments. Data were analysed using "Origin 9" software (OriginLab, Northampton, USA). Differences were considered significant at $p < 0.05$.

4.3. Molecular modeling

4.3.1. Refinement of the human A_{2A} AR and A_1 AR structures

A high-resolution crystal structures of the hA_{2A} AR in complex with ZM241385 was retrieved from the Protein Data Bank (http://www.rcsb.org; pdb code: 5NM4; 1.7-Å resolution [30]). Once removed the fragment of the Soluble Cytochrome b562 contained in the IL3 region, the A_{2A} AR was rebuilt by inserting the IL3 segment and by restoring the wild type receptor sequence (due to the presence of some mutations within the crystallized thermostabilized receptor) with the Homology Modeling tool of MOE [31]. Hydrogen atoms were added and energetically minimized. The crystal structure of the human A_1 AR covalently bound to an antagonist was retrieved from the Protein Data Bank (pdb code: 5UEN; 3.2-Å resolution [35]). Even for this structure, hydrogen atoms were added within MOE and energetically minimized.

4.3.2. Molecular docking analysis

All compound structures were docked into the binding site of the AR structures using three docking tools: the Induced Fit docking protocol of MOE [31], the genetic algorithm docking tool of CCDC Gold [32], and the Lamarckian genetic algorithm of Autodock [33,34]. The Induced Fit docking protocol of MOE is divided into several stages: *Conformational Analysis of ligands*. The algorithm generated conformations from a single 3D conformation by conducting a systematic search. In this way, all combinations of angles were created for each ligand. *Placement*. A collection of poses was generated from the pool of ligand conformations using Alpha Triangle placement method. Poses were generated by superposition of ligand atom triplets and triplet points in the receptor binding site. The receptor site points are alpha sphere centers which represent locations of tight packing. At each iteration, a random conformation was selected, a random triplet of ligand atoms and a random triplet of alpha sphere centres were used to determine the pose. *Scoring*. Poses generated by the placement methodology were scored using the *Alpha HB* scoring function, which combines a term measuring the geometric fit of the ligand to the binding site and a term measuring hydrogen bonding effects. *Induced Fit*. The generated docking conformations were subjected to energy minimization within the binding site and the protein sidechains are included in the refinement stage. In detail, the protein backbone is set as rigid while the side chains are not set to "free to move" but are set to "tethered", where an atom tether is a distance restraint that restrains the distance not between two atoms but between an atom and a fixed point in space. *Rescoring*. Complexes generated by the Induced Fit methodology stage were scored using the *Alpha HB* scoring function. Gold tool was used with default efficiency settings through MOE interface, by selecting GoldScore as scoring function [32]. For the analysis with Autodock (version 4.2.6), we chose lamarckian genetic algorithm with the following settings: 50 runs for each ligand; 2,500,000 as maximum number of energy evaluations; 27,000 as maximum number of generations; 0.02 as rate of gene mutation and 0.8 as rate of crossover. The grid box was set with 50, 50, and 50 points in the $\times$,y, and z directions, respectively, with the default grid spacing of 0.375 Å [33,34].

Acknowledgements

The work was financially supported by the Italian Ministry for University and Research (MIUR, PRIN 2010-2011, 20103W4779_004 project) and the University of Florence (Research Fund 2017).

References

[1] B.B. Fredholm, A.P. IJzerman, K.A. Jacobson, K.N. Klotz, J. Linden, International union of Pharmacology XXV. Nomenclature and classification of adenosine receptors, Pharmacol. Rev. 53 (2001) 527–552.
[2] B.B. Fredholm, A.P. IJzerman, K.A. Jacobson, J. Linden, C.E. Muller, International union of Pharmacology LXXXI. Nomenclature and classification of adenosine receptors. An up date, Pharmacol. Rev. 63 (2011) 1–34.
[3] R.A. Cunha, Neuroprotection by adenosine in the brain: from A_1 receptor activation to A_{2A} receptor blockade, Purinergic Signal. 1 (2005) 111–134.
[4] J. Stockwell, E. Jackova, F.S. Cayabyab, Adenosine A_1 and A_{2A} receptors in the brain: current research and their role in neurodegeneration, Molecules 22 (2017) 676.
[5] Z. Chen, J. Stockwell, F.S. Cayabyab, Adenosine A_1 receptor-mediated endocytosis of AMPA receptors contributes to impairments in long-term potentiation (LTP) in the middle-aged rat hippocampus, Neurochem. Res. 41 (2016) 1085–1097.
[6] J. Stockwell, Z. Chen, M. Niazi, S. Nosib, F.S. Cayabyab, Protein phosphatase role in adenosine A_1 receptor-induced AMPA receptor trafficking and rat hippocampal neuronal damage in hypoxia/reperfusion injury, Neuropharmacology 102 (2016) 254–265.
[7] P.A. Borea, S. Gessi, S. Merighi, F. Vincenzi, K. Varani, Pharmacology of adenosine receptors: the state of art, Physiol. Rev. 98 (2018) 1591–1625.
[8] R. Franco, G. Navarro, Adenosine A_{2A} receptor antagonist in neurodegenerative diseases: huge potential and huge challenges, Front. Psychiatry 9 (2018) 68.
[9] M. Rivera-Oliver, M. Díaz-Ríos, Using caffeine and other adenosine receptor antagonists and agonists as therapeutic tools against neurodegenerative diseases: a review, Life Sci. 101 (2014) 1–9.
[10] K. Xu, D.G. Di Luca, M. Orrù, Y. Xu, J.-F. Chen, M.A. Schwarzschild, Neuroprotection by caffeine in the MPTP model of Parkinson's disease and its dependence on adenosine A_{2A} receptors, Neuroscience 322 (2016) 129–137.
[11] M.H. Eskelinena, M. Kivipelto, Caffeine as a protective factor in dementia and Alzheimer's disease, J. Alzheimer's Dis. 20 (2010) S167–S174.
[12] M. Kolahdouzan, M.J. Hamadeh, The neuroprotective effects of caffeine in neurodegenerative diseases, CNS Neurosci. Ther. 23 (2017) 272–290.
[13] O.P. Dall'Igna, L.O. Porciuncula, D.O. Souza, R.A. Cunha, Neuroprotection by caffeine and adenosine A_{2A} receptor blockade of β-amyloid neurotoxicity, British J. Pharmacol. 138 (2003) 1207–1209.
[14] O.P. Dall'Igna, P. Fett, M.W. Gomes, D.O. Souza, R.A. Cunha, D.R. Lara, Caffeine and adenosine A_{2A} receptor antagonist prevent β-amyloid (25–35)-induced cognitive deficits in mice, Exp. Neurol. 203 (2007) 241–245.
[15] E. Faivre, J.E. Coelho, K. Zornbach, E. Malik, Y. Baqi, M. Schneider, L. Cellai, K. Carvalho, S. Sebda, M. Figeac, S. Eddarkaoui, R. Caillierez, Y. Chern, M. Heneka, N. Sergeant, C.E. Müller, A. Halle, L. Buée, L.V. Lopes, D. Blum, Beneficial effect of a selective adenosine A_{2A} receptor antagonist in the APPswe/PS1dE9 mouse model of Alzheimer's disease, Front. Mol. Neurosci. 11 (2018) 235.
[16] S. Giunta, V. Andriolo, A. Castorina, Dual blockade of the A_1 and A_{2A} adenosine receptor prevents amyloid beta toxicity in neuroblastoma cells exposed to aluminium chloride, Int. J. Biochem. Cell Biol. 5 (2014) 122–136.
[17] L. Squarcialupi, V. Colotta, D. Catarzi, F. Varano, M. Betti, K. Varani, F. Vincenzi, P.A. Borea, N. Porta, A. Ciancetta, S. Moro, 7-Amino-2-phenylpyrazolo[4,3-d]pyrimidine derivatives: structural investigations at the 5-position to target al and A2A adenosine receptors. Molecular modeling and pharmacological studies, Eur. J. Med. Chem. 84 (2014) 614–627.
[18] L. Squarcialupi, M. Falsini, D. Catarzi, F. Varano, M. Betti, K. Varani, F. Vincenzi, D. Dal Ben, C. Lambertucci, R. Volpini, V. Colotta, Exploring the 2- and 5-positions of the pyrazolo[4,3-*d*]pyrimidin-7-amino scaffold to target human A_1 and A_{2A} adenosine receptors, Bioorg. Med. Chem. 24 (2016) 2794–2808.
[19] F. Varano, D. Catarzi, F. Vincenzi, M. Betti, M. Falsini, A. Ravani, P.A. Borea,

V. Colotta, K. Varani, Design, synthesis, and pharmacological characterization of 2-(2-furanyl)thiazolo[5,4-*d*]pyrimidine-5,7-diamine derivatives: New highly potent A_{2A} adenosine receptor inverse agonists with antinociceptive activity, J. Med. Chem. 59 (2016) 10564–10576.

[20] L. Squarcialupi, M. Betti, D. Catarzi, F. Varano, M. Falsini, A. Ravani, S. Pasquini, F. Vincenzi, V. Salmaso, M. Sturlese, K. Varani, S. Moro, V. Colotta, The role of 5-arylalkylamino- and 5-piperazino- moieties on the 7-aminopyrazolo[4,3-*d*]pyrimidine core in affecting adenosine A_1 and A_{2A} receptor affinity and selectivity profiles, J. Enzyme Inhib. Med. Chem. 32 (2017) 248–263.

[21] M. Falsini, L. Squarcialupi, D. Catarzi, F. Varano, M. Betti, D. Dal Ben, G. Marucci, M. Buccioni, R. Volpini, T. De Vita, A. Cavalli, V. Colotta, The 1,2,4-triazolo[4,3-a]pyrazin-3-one as a versatile scaffold for the design of potent adenosine human receptor antagonists. Structural investigations to target the A_{2A} receptor, J. Med. Chem. 60 (2017) 5772–5790.

[22] S. Gessi, S. Bencivenni, E. Battistello, F. Vincenzi, V. Colotta, D. Catarzi, F. Varano, S. Merighi, P.A. Borea, K. Varani, Inhibition of A_{2A} adenosine receptor signaling in cancer cells proliferation by the novel antagonist TP455, Front. Pharmacol. 8 (2017) 888.

[23] D. Catarzi, F. Varano, M. Falsini, K. Varani, F. Vincenzi, V. Colotta, Development of novel pyridazinone-based adenosine receptor ligands, Bioorg. Med. Chem. Lett. 28 (2018) 1484–1489.

[24] F. Varano, D. Catarzi, M. Falsini, F. Vincenzi, S. Pasquini, K. Varani, V. Colotta, Identification of novel thiazolo[5,4-d]pyrimidine derivatives as human A_1 and A_{2A} adenosine receptor antagonists/inverse agonists, Bioorg. Med. Chem. 26 (2018) 3688–3695.

[25] F. Varano, D. Catarzi, F. Vincenzi, M. Falsini, S. Pasquini, P.A. Borea, V. Colotta, K. Varani, Structure-activity relationship studies and pharmacological characterization of N5-heteroarylalkyl-substituted-2-(2-furanyl)thiazolo[5,4-d]pyrimidine-5,7-diamine-based derivatives as inverse agonists at human A_{2A} adenosine receptor, Eur. J. Med. Chem. 155 (2018) 552–561.

[26] D. Preti, P.G. Baraldi, A.R. Moorman, P.A. Borea, K. Varani, History and perspective of A_{2A} adenosine receptor antagonists as potential therapeutic agents, Med. Res. Rev. 35 (2015) 790–848.

[27] L. Di Cesare Mannelli, M. Zanardelli, P. Failli, C. Ghelardini, Oxaliplatin-induced oxidative stress in nervous system-derived cellular models: could it correlate with in vivo neuropathy? Free Radic. Biol. Med. 61 (2013) 143–150.

[28] J. Faria, J. Barbosa, O. Queirós, R. Moreira, F. Carvalho, R.J. Dinis-Oliveira, Comparative study of the neurotoxicological effects of tramadol and tapentadol in SH-SY5Y cells, Toxicology 359 (2016) 1–10.

[29] J.J.V. Branca, G. Morucci, M. Maresca, B. Tenci, R. Cascella, F. Paternostro, C. Ghelardini, M. Gulisano, L. Di Cesare Mannelli, A. Pacini, Selenium and zinc: Two key players against cadmium-induced neuronal toxicity, Toxicol. In Vitro 48 (2018) 159–169.

[30] T. Weinert, N. Olieric, R. Cheng, S. Brunle, D. James, D. Ozerov, D. Gashi, L. Vera, M. Marsh, K. Jaeger, F. Dworkowski, E. Panepucci, S. Basu, P. Skopintsev, A.S. Dore, T. Geng, R.M. Cooke, M. Liang, A.E. Prota, V. Panneels, P. Nogly, U. Ermler, G. Schertler, M. Hennig, M.O. Steinmetz, M. Wang, J. Standfuss, Serial millisecond crystallography for routine room-temperature structure determination at synchrotrons, Nat. Commun. 8 (2017) 542.

[31] I. Molecular Operating Environment; C.C.G., 1255 University St., Suite 1600, Montreal, Quebec, Canada, H3B 3X3.

[32] G. Jones, P. Willett, R.C. Glen, A.R. Leach, R. Taylor, Development and validation of a genetic algorithm for flexible docking, J. Mol. Biol. 267 (1997) 727–748.

[33] G.M. Morris, D.S. Goodsell, R.S. Halliday, R. Huey, W.E. Hart, R.K. Belew, A.J. Olson, Automated docking using a Lamarckian genetic algorithm and an empirical binding free energy function, J. Comput. Chem. 19 (1998) 1639–1662.

[34] G.M. Morris, R. Huey, W. Lindstrom, M.F. Sanner, R.K. Belew, D.S. Goodsell, A.J. Olson, AutoDock4 and AutoDockTools4: automated docking with selective receptor flexibility, J. Comput. Chem. 30 (2009) 2785–2791.

[35] A. Glukhova, D.M. Thal, A.T. Nguyen, E.A. Vecchio, M. Jorg, P.J. Scammells, L.T. May, P.M. Sexton, A. Christopoulos, Structure of the adenosine A_1 receptor reveals the basis for subtype selectivity, Cell 168 (2017) 867–877 e813.

[36] G. La Regina, R. Bai, W. Rensen, A. Coluccia, F. Piscitelli, V. Gatti, A. Bolognesi, A. Lavecchia, I. Granata, A. Porta, B. Maresca, A. Soriani, M.L. Iannitto, M. Mariani, A. Santoni, A. Brancale, C. Ferlini, G. Dondio, M. Varasi, C. Mercurio, E. Hamel, P. Lavia, E. Novellino, R. Silvestri, Design and synthesis of 2-heterocyclyl-3-arylthio-1H-indoles as potent tubulin polymerization and cell growth inhibitors with improved metabolic stability, J. Med. Chem. 54 (2011) 8394–8406.

[37] E. Bellale, M. Naik, V. VB, A. Ambady, A. Narayan, V. SRavishankar, P. Ramachandran, R. Kaur, J. McLaughlin, S. Whiteaker, S. Morayya, S. Guptha, A. Sharma, D. Raichurkar, V. Awasthy, P. Achar, B. Vachaspati, M. Bandodkar, M. Panda, Chatterji Diarylthiazole: an antimycobacterial scaffold potentially targeting PrrB-PrrA two-component system, J. Med. Chem. 57 (2014) 6572–6582.

[38] G.A. Bennett, G.B. Mullen, J.T. Mitchell, W.E. Jones, S.D. Allen, C.R. Kinsolving, V. St Georgiev, Studies on antifungal agents 30. Novel substituted 3-(2-furanyl)-3-(1H-imidazol-1-ylmethyl)-2-methyl-5-phenyl(or phenyloxymethy)-isoxazolidines, Eur. J. Med. Chem. 24 (1989) 579–583.

[39] N. Saldabol, Yu. Popelis, V. Shatz, V. Slavinskaya, Bromination of 2-acetyl-5-methylfuran, Chem. Heterocycl. Compd. 35 (1999) 161–163.

[40] A. Thomas, M. Buccioni, D. Dal Ben, C. Lambertucci, G. Marucci, C. Santinelli, A. Spinaci, S. Kachler, K.N. Klotz, R. Volpini, The length and flexibility of the 2-substituent of 9-ethyladenine derivatives modulate affinity and selectivity for the human A_{2A} adenosine receptor, ChemMedChem 11 (2016) 1829–1839.

[41] M. Buccioni, C. Santinelli, P. Angeli, D. Dal Ben, C. Lambertucci, A. Thomas, R. Volpini, G. Marucci, Overview on radiolabel-free in vitro assays for GPCRs, Mini – Rev. Med. Chem. 17 (2017) 3–14.

[42] M. Buccioni, G. Marucci, D. Dal Ben, D. Giacobbe, C. Lambertucci, L. Soverchia, A. Thomas, R. Volpini, G. Cristalli, Innovative functional cAMP assay for studying G protein-coupled receptors: application to the pharmacological characterization of GPR17, Purinergic Signal 7 (2011) 463–468.